

## Article

# Exploration of CYP4B1 Substrate Promiscuity Across Three Species

Annika Röder <sup>1</sup>, Michael C. Hutter <sup>2</sup>, Eva Heitzer <sup>1</sup>, Pia Josephine Franz <sup>1</sup>, Saskia Hüsken <sup>3</sup>, Constanze Wiek <sup>3</sup> and Marco Girhard <sup>1,\*</sup>

<sup>1</sup> Institute of Biochemistry, Heinrich Heine University, 40225 Düsseldorf, Germany; annika.roeder@hhu.de (A.R.); eva.heitzer@hhu.de (E.H.); pifra102@uni-duesseldorf.de (P.J.F.)

<sup>2</sup> Center for Bioinformatics, Saarland University, Campus Building E2.1, 66123 Saarbruecken, Germany

<sup>3</sup> Department of Otorhinolaryngology and Head/Neck Surgery, Heinrich Heine University, 40225 Düsseldorf, Germany; constanze.wiek@med.uni-duesseldorf.de (C.W.)

\* Correspondence: marco.girhard@hhu.de

**Abstract:** Enzymes of the cytochrome P450 monooxygenase family 4 (CYP4) in mammals are generally involved either in endobiotic metabolism (e.g., acting on fatty acids or eicosanoids), or the modification of xenobiotics including therapeutic drugs. CYP4B1 is special, as it is an enigmatic enzyme acting at the interface between xenobiotic and endobiotic metabolism. However, a systematic analysis of CYP4B1's substrate scope has not yet been reported. Herein, a three-step approach to identify novel substrates for three CYP4B1 orthologs (namely from rabbits, green monkeys, and mouse lemurs) is described. First, screening of a library containing 502 natural products revealed potential novel substrate groups for CYP4B1. Second, based on these results, a systematic library was defined consisting of 63 compounds representing 10 compound groups. Third, in vitro conversion of these compounds by CYP4B1 and identification of conversion products were conducted, supported by in silico docking, allowing the prediction of binding probabilities and potential oxidation sites. We report five new substrate groups (acyclic, monocyclic and bicyclic terpenoids, stilbenoids, and vanilloids), twenty-eight new substrates (inter alia capsaicin, gingerol, genistein, stilbene, myristicin, thioanisole), and two new reaction types for CYP4B1 (S-oxidation, O-demethylation). Consequently, CYP4B1 is a far more promiscuous enzyme than previously thought.

**Keywords:** CYP4B1; capsaicin; gingerol; genistein; stilbene; resveratrol; geraniol; nerol; carvone; S-oxidation



Academic Editor: Zhen Li

Received: 25 March 2025

Revised: 30 April 2025

Accepted: 4 May 2025

Published: 7 May 2025

**Citation:** Röder, A.; Hutter, M.C.; Heitzer, E.; Franz, P.J.; Hüsken, S.; Wiek, C.; Girhard, M. Exploration of CYP4B1 Substrate Promiscuity Across Three Species. *Catalysts* **2025**, *15*, 454. <https://doi.org/10.3390/catal15050454>

**Copyright:** © 2025 by the authors. Licensee MDPI, Basel, Switzerland. This article is an open access article distributed under the terms and conditions of the Creative Commons Attribution (CC BY) license (<https://creativecommons.org/licenses/by/4.0/>).

## 1. Introduction

Cytochrome P450 monooxygenases (P450s) are heme-thiolate enzymes found in all domains of life and even in viruses [1,2]. With more than 1,000,000 known sequences so far, they constitute one of the largest enzyme superfamilies [2]. In general, P450s catalyze a wide variety of oxidative reactions through the reductive activation of molecular oxygen, with the hydroxylation of non-activated C-H bonds in organic substrates as the most prevalent reaction [3]. Beyond this primary function, other reactions commonly catalyzed by P450s include epoxidation of C=C double bonds, N- and S-oxidation, and N-, O-, or S-dealkylation [3,4]. A defining feature of P450s is their ability to operate with high stereospecificity and regioselectivity, allowing precise control of reaction pathways [5,6]. Thus, in drug development, they facilitate selective biotransformations to optimize drug metabolites or synthesize bioactive compounds [7].

P450s are divided into families according to their sequence identity, so that the number following the term 'CYP' indicates the family in which the enzymes share > 40% sequence identity with each other [8]. The mammalian CYP4 family, whose members are highly conserved throughout evolution, evolved approximately 1.25 million years ago and is therefore one of the oldest families [9,10]. Thirteen CYP4 proteins are known in humans, which fall into six subfamilies, namely 4A, 4B, 4F, 4V, 4X, and 4Z [9]. Enzymes of the CYP4 family are generally involved either in endobiotic metabolism, mostly associated with  $\omega$ -hydroxylation of fatty acids and the metabolism of signaling molecules, or in the modification of xenobiotics and therapeutic drugs in mammals [11,12].

CYP4B1 is special in this group (together with CYP4A11) because it accepts typical endobiotic substrates and also plays a role in the activation of xenobiotics [11,13]. Endogenous substrates described so far include saturated fatty acids, fatty alcohols (*n*-alkanols), and *n*-alkanes, which are modified through hydroxylation, mainly on terminal and subterminal positions [13–15]. A key example of xenobiotic substrates is the so-called 'hallmark' substrate of CYP4B1, 4-ipomeanol (4-IPO), a furan derivative produced by sweet potatoes (*Ipomoea batatas*) as a defense mechanism against fungal infections with *Fusarium solani* [16]. First identified in the 1970s, 4-IPO gained attention after cattle consuming mold-infected sweet potatoes developed pulmonary edema and respiratory distress and died as a result [17]. Subsequent animal and in vitro studies identified CYP4B1, which is predominantly expressed in the lung, as responsible for the activation of 4-IPO to its reactive DNA binding metabolite by initial epoxidation of its furan group [18–21]. Further described xenobiotic substrates include other furan-containing compounds such as perilla ketone (PK), which is found in the essential oil of the mint plant *Perilla frutescens* [18,22] as well as other synthetic compounds comprising 2-furylpentyl ketone, 2-pentylfuran, 2-hexylfuran, and *N*-alkyl-3-furancarboxamides [23,24]. Other exogenous substrates include the anticonvulsant valproic acid [25,26], the gut microbial fermentation product, 3-methylindole (3-MI) [23], and the aromatic compounds 2-aminoanthracene (2-AA) and cumene [23,27].

These unique metabolic capabilities highlight CYP4B1's involvement in both physiological processes and its potential application in targeted therapies, such as suicide gene systems [24,28]. However, a systematic analysis of CYP4B1's substrate scope has not been conducted so far and therefore it remains incomplete.

One reason for the incomplete investigation of CYP4B1's substrate scope might be the fact that the human ortholog does not play a role in the human metabolic network, since it has undergone evolutionary changes that render it catalytically inactive. Specifically, a unique proline-to-serine substitution at position 427 (p.P427S) in the meander region of the human CYP4B1 disrupts its catalytic function, distinguishing it from its active counterparts in other species, such as rodents and rabbits that exhibit catalytic activity [29,30]. This evolutionary inactivation has positioned human CYP4B1 as an 'orphan' enzyme with an unclear physiological role, despite its conservation across species. Consequently, the paramount studies referring to human CYP4B1 are focused on its gene regulation and mRNA levels [31,32]. Although it has no catalytic activity, mRNA levels of the human enzyme can be found in extrahepatic tissues, mainly in lung tissue, which is altered in tumor cells and thus associated with the development of and/or response to cancer [31–35].

To approximate the pristine catalytical function of human CYP4B1, we have chosen two CYP4B1 orthologs from closely related primates (sequences available in public databases), namely the green monkey from the Old World monkey family (chCYP4B1, *Chlorocebus sabaeus*, XM007978860.2) and the gray mouse lemur from the prosimian family (mlCYP4B1; *Microcebus murinus*, XM\_012776101.1). These orthologs were chosen because they have a substantially higher sequence identity to the human CYP4B1 ortholog than the rabbit one

(up to 95%) and contain a p.P427 (not the p.P427S substitution). Initial experiments with lauric acid as the benchmark substrate revealed that both orthologs are catalytically active and exceeded activity of rabbit CYP4B1 (rCYP4B1)—so far the best-investigated ortholog.

Herein, we report a systematic three-step approach to investigate the substrate scope of CYP4B1 across the aforementioned two non-human primate orthologs in comparison to rCYP4B1. First, the identification of promising new substance groups was based on initiation of spectral changes indicating binding; second, representative compounds for each group were compiled in a systematic library; and third, *in vitro* conversion of all compounds and the identification of the respective conversion products were carried out. In addition, *in silico* docking was applied to assist the identification of potential reaction sites from the respective GC/MS, LC/MS or LC/MS/MS data.

## 2. Results and Discussion

### 2.1. Screening of a Natural Product Library for Spectral Changes Indicating Substrate Binding

Binding of substrates to the heme iron of a P450 is often accompanied by displacing the water ligand and the induction of a shift of the ferric heme iron from a low-spin to a high-spin state, altering its electronic configuration. This transition can be monitored in cytochrome P450 spectra as a so-called type I shift, with a Soret absorption minimum near 420 nm and a maximum around 390 nm [36,37]. Since binding of a compound to the P450 is a necessary requirement for its catalytic conversion, monitoring of spectral changes indicating potential binding to CYP4B1 can be used as first step for fast screening of large compound libraries to identify potential novel substrates.

Here, a blinded screening of a commercial natural product library (502 compounds; Supplementary Table S1) was conducted in 96-well microwell plates with rCYP4B1 and mCYP4B1. Out of the 502 compounds tested, 65 indicated a visible spectral shift with rCYP4B1, and 56 with mCYP4B1 (summarized in Supplementary Table S1). Unblinding of the library revealed repeated ‘hits’ for flavones, flavonoids, vanilloids, and structurally related compounds, resulting in a pattern that emphasized these groups as the most promising ones for subsequent screening. For instance, quercetin **54**, which is a representative compound of flavonoids, exhibited a distinct maximum at 390 nm and minimum at 420 nm with both rCYP4B1 and mCYP4B1. Some vanilloids, such as piperine **50** and gingerol **49**, induced spectral changes with mCYP4B1, but not with rCYP4B1. Conversely, myristicin **41** induced spectral changes in the screening with rCYP4B1, but not in mCYP4B1.

In summary, these results already suggested potential differences in substrate binding preferences between the two chosen orthologs, indicating the necessity to include catalytically active CYP4B1 orthologs with a close relation to the human one.

### 2.2. Definition of a Systematic Compound Library for *In Vitro* Conversion

A systematic substrate library was defined, consisting of 63 organic compounds that were divided into 10 groups based on their structural properties (Figure 1). Groups I and II consist of saturated fatty acids and *n*-alkanols, respectively, which are well investigated substrates for rCYP4B1 [14]. They were included in order to identify potential differences across species with respect to activity and hydroxylation patterns (e.g.,  $\omega$ : $\omega$ -1 ratio) by chCYP4B1 and mCYP4B1. Groups III to X contained compounds that had so far not been described as being metabolized by CYP4B1 (with a few exceptions in groups VI and VII). Therefore, the following requirements were defined: (i) the compound has been described in the literature as being metabolized by a P450 enzyme; either (ii) a spectral change was observed for the respective compound within the initial screening of the natural product library, or (iii) the compound is structurally related to that particular compound, but was not part of the natural product library (e.g., *trans*-Stilbene **42** was included, because spectral

changes were frequently observed for structurally related isoflavones and flavones, such as 7-hydroxyflavone 56).

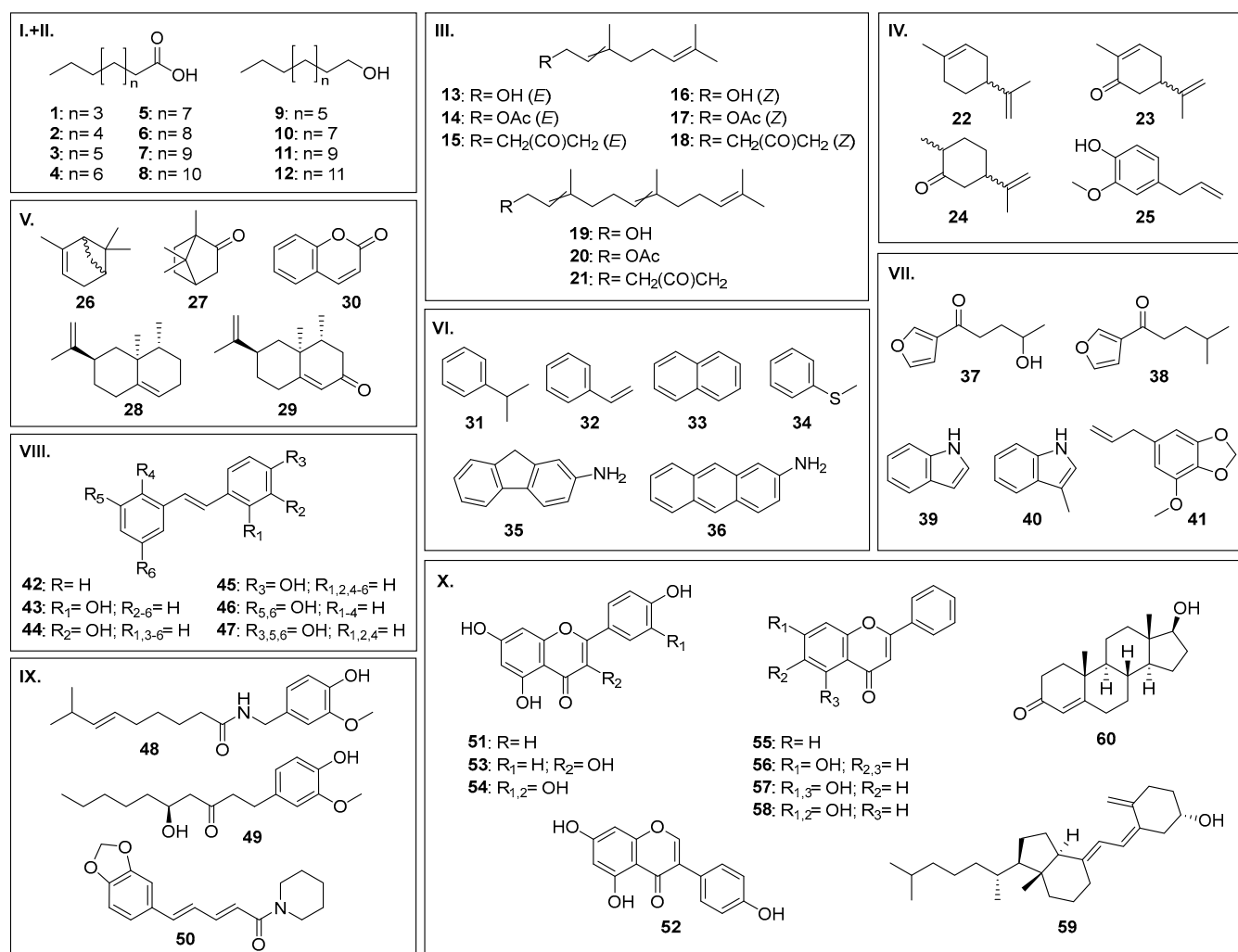


**Figure 1.** CYP4B1 compound library for in vitro screening. 63 compounds were divided into 10 groups (I–X.) as described in chapter 2.2. For 22, 23 and 26 enantiopure compounds were included: (R)-(+)-limonene 22a, (S)-(–)-limonene 22b; (R)-(–)-carvone 23a, (S)-(+)-carvone 23b; (1R)-(+)- $\alpha$ -pinene 26a, (1S)-(–)- $\alpha$ -pinene 26b.

For each compound of the library in vitro conversion was conducted with the three CYP4B1 orthologs, and the identification of potential binding sites was supported by computational docking. This allowed us to study species differences in catalytic activity and chemoselectivity of these CYP4B1 enzymes. The results for each group are described in the following sections; all results of the in vitro screening are summarized in Section 2.3.9.

### 2.3. In Vitro Conversion of Library Compounds

#### 2.3.1. Group I and II: Saturated Fatty Acids and n-Alkanols

Saturated fatty acids with chain lengths C9–C16 1–8 (C9–C16-FA) and *n*-alkanols 9–12 (C10–C16-ol) are well-investigated substrates for rCYP4B1 [14]. Here, we compared the activity and hydroxylation patterns of rCYP4B1 with those of chCYP4B1 and mlCYP4B1. For rCYP4B1, the highest activity was observed towards C11–3 (52%) and C12-FA 4 (50%) and a decrease in activity towards longer and shorter chain lengths (Figure 2). In contrast, both primate orthologs showed the highest conversion with C12-FA 4 (85%) and C13-FA 5 (78% for chCYP4B1 and 67% for mlCYP4B1). In comparison to rCYP4B1, the activities for

FAs with shorter chain lengths were lower, but they were higher in the case of C14-FA 6 (48% and 32%) and C15-FA 7. In conclusion, the activities for both primate orthologs are shifted towards longer chain lengths compared to rCYP4B1.

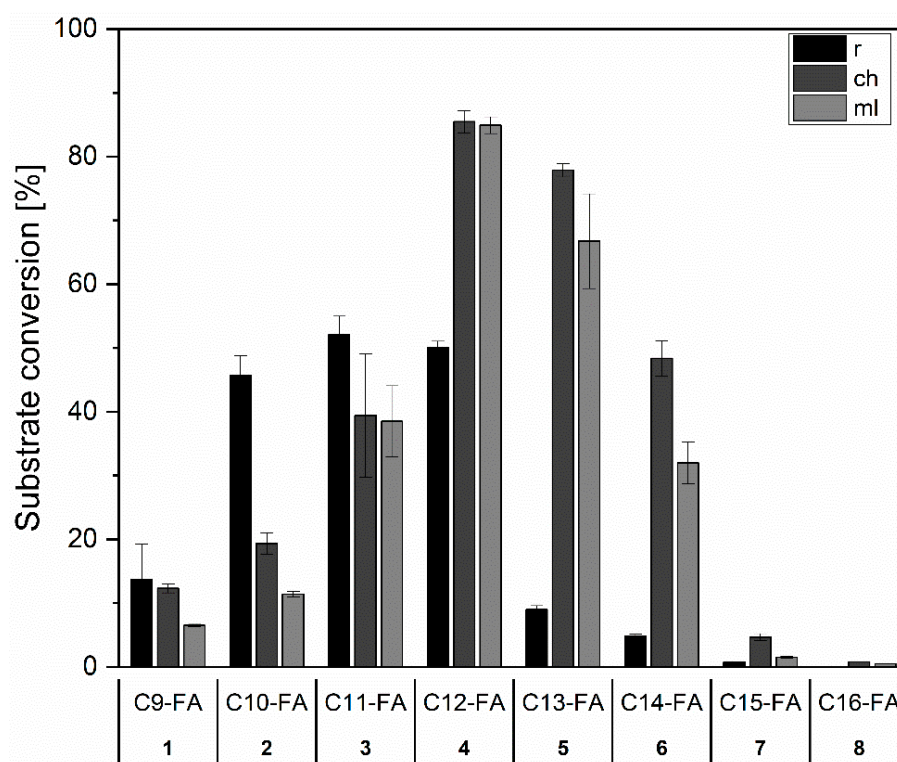


**Figure 2.** Substrate conversion of C9-C16-FA 1–8 using rCYP4B1, chCYP4B1 and mlCYP4B1. Mean substrate depletion [%] and standard deviation after 90 min incubation is calculated for at least three independent experiments.

For all chain lengths, the main products formed were  $\omega$ - and  $\omega$ -1-hydroxylated fatty acids, which is in line with previous reports on rCYP4B1 [14]. However, particularly in the case of C11-FA 3 and C12-FA 4, strong differences in hydroxylation patterns (product distributions) between the orthologs were observed (summarized in Supplementary Table S2): rCYP4B1 forms seven products resulting from hydroxylations at positions  $\omega$ ,  $\omega$ -1,  $\omega$ -2 on the alkyl chain side, as well as  $\alpha$ ,  $\beta$ ,  $\gamma$ , and  $\delta$  on the carboxyl group side (Figure 3). The  $\omega$ : $\omega$ -1 ratio for C12-FA 4 with rCYP4B1 was 1.3, but for mlCYP4B1 the product distribution was markedly different. There,  $\omega$ -hydroxylation accounted for ~90% of the observed products, while positions  $\omega$ -1 and  $\alpha$  were hydroxylated to a small extent and only traces of  $\gamma$ - and  $\delta$ -hydroxylated products were observed (Figure 3). Consequently, the  $\omega$ : $\omega$ -1 ratio was 13 (10 $\times$  higher compared to rCYP4B1). For chCYP4B1, an  $\omega$ : $\omega$ -1 ratio of 8 was obtained with C12-FA 4 (6 $\times$  higher compared to rCYP4B1). The observed increased regioselectivity for  $\omega$ -hydroxylation suggests that the architecture of the active center is altered in both primate orthologs, but comparison of the homology models generated from the rCYP4B1 crystal structure implies that the only structural difference in the binding pocket is due to an exchange of isoleucine 221 (rCYP4B1) with leucine in chCYP4B1 (p.I221L), and with methionine in mlCYP4B1 (p.I221M), respectively. Although this position is rather far away from the heme (17.9 Å distance between C $\beta$  and the iron), it seemingly affects the binding of fatty acids. The different spatial extension of the isoleucine, leucine, and methionine side chains causes changes in the orientation of the bound ligands despite the lack of hydrogen-bonding between the substrate and any of these side chains (see also Section 2.3.7).

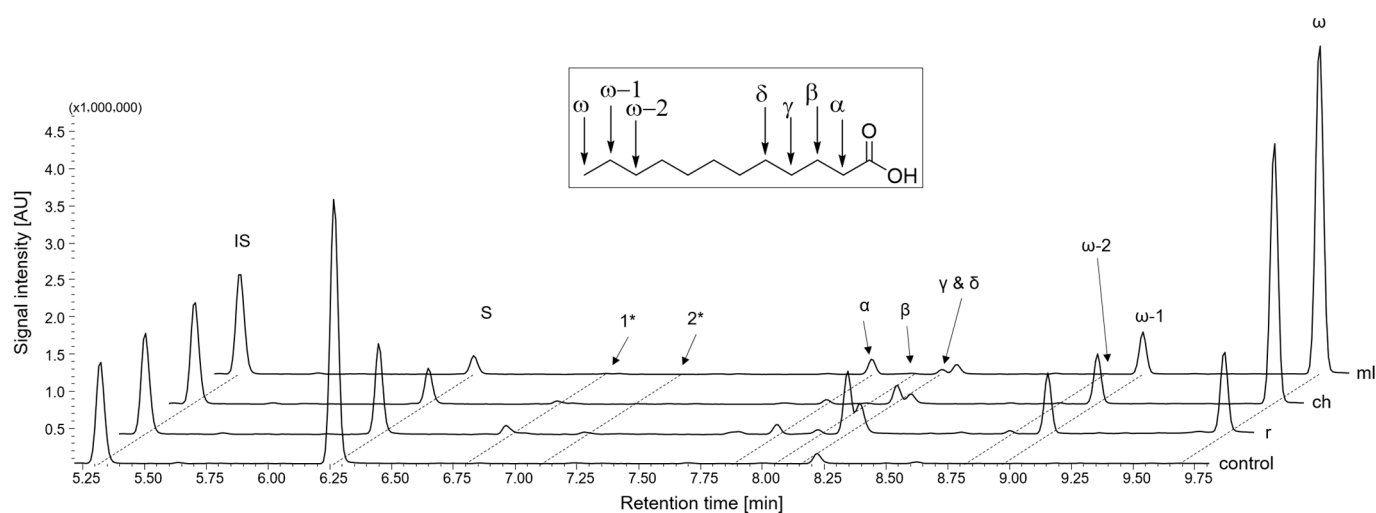


**Figure 3.** GC/MS chromatograms of C12-FA 4 conversion. Comparison between rCYP4B1 (r), chCYP4B1 (ch), mlCYP4B1 (ml), and a reaction without P450 (control). The inset indicates the observed hydroxylation positions of C12-FA 4 that are also pointed out in the GC/MS chromatograms. 1\* and 2\*: non-enzymatically formed lactones originating from  $\gamma$ - and  $\delta$ -hydroxylated products, S: substrate C12-FA 4, IS: internal standard.

For *n*-alkanols 9–12, the conversion is generally lower compared to FAs 1–8. However, a similar trend regarding the preferred chain lengths between the orthologs is visible: The highest conversion with rCYP4B1 was observed for C12-ol 10 (18%), but C14-ol 11 with chCYP4B1 and mlCYP4B1 (15% and 18%, respectively). All four *n*-alkanols were hydroxylated at the  $\omega$ -position, but to different extents (summarized in Supplementary Table S3). In the case of C12-ol 10, the  $\omega$ -1 product was formed additionally, while for C14-ol 11,  $\omega$ -1 hydroxylation was the main product for all three orthologs, with the  $\omega$ - and  $\omega$ -2 products as byproducts.

In silico docking suggests that the carbon chain of longer *n*-alkanols (as well as fatty acids) is compressed and folded within the binding pocket, thus exposing positions other than both ends to the heme iron, which is in line with previous results for rCYP4B1 [14].

### 2.3.2. Group III: Acyclic Terpenoids

Terpenes and terpenoids are natural compounds responsible for various scents of plant oils. In general, terpenes are composed of isoprene units and terpenoids contain additional heteroatoms. Both occur naturally in acyclic and cyclic conformations. Their use as volatile ingredients in cosmetics and perfumes leads to daily exposure to respiratory enzymes such as CYP4B1, which makes them applicable as potential substrates [38].

Group III contains the acyclic terpenoids geraniol 13 and nerol 16 (*E/Z* diastereomers with two isoprene units), and farnesol 19 (three isoprene units), as well as their respective acetate esters (14, 17, and 20) and acetyl derivatives (15, 18, and 21).

Remarkably, all CYP4B1 orthologs converted all compounds built of two isoprene units (13–18), whereas compounds 19–21 with three isoprene units were not converted by any ortholog. Conversion of geraniol 13 was generally higher than for nerol 16. If one compares the activities of the different orthologs for 13 and 16, chCYP4B1 and rCYP4B1 are similar, but slightly higher than those of mlCYP4B1.

Both geraniol 13 and nerol 16 were exclusively hydroxylated at the terminal position, resulting in 8-hydroxygeraniol 13-P1 or 8-hydroxynерol 16-P1 as the only product. This strong regioselectivity was also observed by previous studies with bacterial CYP154E1 and CYP154A8 [39,40]. Regarding mammalian P450s, Hagvall et al. described geraniol and

epoxide derivatives as sensitizing products of geraniol catalyzed by CYP1A1 and CYP3A5 when exposed to human skin [41].

The general preference by CYP4B1 of *E*- over *Z*- was also observed when comparing the activities of the three orthologs for the respective acetate esters (**14** and **17**) and acetyl derivatives (**15** and **18**). However, whereas activities for geranyl acetate **14** and geranyl acetone **15** were almost equal for the individual orthologs (e.g., 24% in the case of rCYP4B1), neryl acetate **17** was preferred over neryl acetone **18**, most apparent in the case of chCYP4B1 (42% versus 16%).

The product distribution for the acetate esters (**14** and **17**) and acetyl derivatives (**15** and **18**) of geraniol **13** and nerol **16** was broader: The main products result from epoxidations of the C=C double bonds, but terminal hydroxylation to the 8-hydroxy products was also observed, albeit to lesser extents. Notably, epoxides of geraniol **13** have been demonstrated to be allergens in the context of cutaneous metabolic activation of geraniol **13** in fragrances, and thus it may also be that epoxidation of the acetate esters and acetyl derivatives in the lung leads to allergic reactions [41].

### 2.3.3. Groups IV and V: Monocyclic and Bicyclic Terpenes/Terpenoids

Group IV consists of the monocyclic terpenes (*R*)-(+)-limonene **22a** and (*S*)-(–)-limonene **22b**, and the monocyclic terpenoids eugenol **25**, (*R*)-(–)-carvone **23a**, (*S*)-(+)-carvone **23b**, and dihydrocarvone **24** (mixture of diastereomers).

Within group IV, (*R*)-(–)-carvone **23a** and (*S*)-(+)-carvone **23b**, as well as dihydrocarvone **24**, were converted by all three orthologs. In all cases, rCYP4B1 showed the highest activity, followed by chCYP4B1 and mCYP4B1; and all orthologs preferred (*R*)-carvone **23a** over (*S*)-carvone **23b**. In nature, carvone **23** functions as a precursor of limonene **22**, for which no conversion by CYP4B1 was observed. Shimada et al. studied limonene **22** and carvone **23** metabolism in different animal species including rabbits and humans, and observed that both were accepted by liver P450s such as CYP1A2 and CYP2B4, forming carveol, carvone **23**, and perillyl alcohol after incubation with limonene **22**, and likewise carveol after incubation with carvone **23**, with CYP2C enzymes as the most responsible P450s [42]. In contrast, GC/MS analysis of carvone **23** conversions by CYP4B1 indicated three hydroxylated and/or epoxidized products (*m/z* +16) of carvone (*R/S*) **23**, as well as dihydrocarvone **24** and products of dihydrocarvone **24** (Figure 4). The obtained orientation from docking points towards a reaction involving the C=C double bond of the isopropenyl group in all three orthologs, suggesting 7,8-carvone oxide as one product. Notably, dihydrocarvone **24** was probably formed from carvone **23** by unknown endogenous *E. coli* proteins present in the soluble protein of the reaction mixture rather than CYP4B1, which was also observed by Yoshida et al. as a by-product of carvone **23** production in *E. coli* [43]. Nevertheless, dihydrocarvone **24** itself was accepted as a substrate by all three CYP4B1 orthologs, resulting in five hydroxylated and/or epoxidized products (*m/z* +16) (Figure 4). Again, the docking results suggest a reaction at the C=C double bond of the isopropenyl group to form 7,8-dihydrocarvone oxide.

In group V, six representatives of bicyclic terpenes/terpenoids are included: (*R*)-(+)- $\alpha$ -pinene **26a**, (*S*)-(–)- $\alpha$ -pinene **26b**, and valencene **28** belong to the bicyclic terpenes, and camphor **27**, nootkatone **29**, and coumarin **30** built the selection of the bicyclic terpenoids.

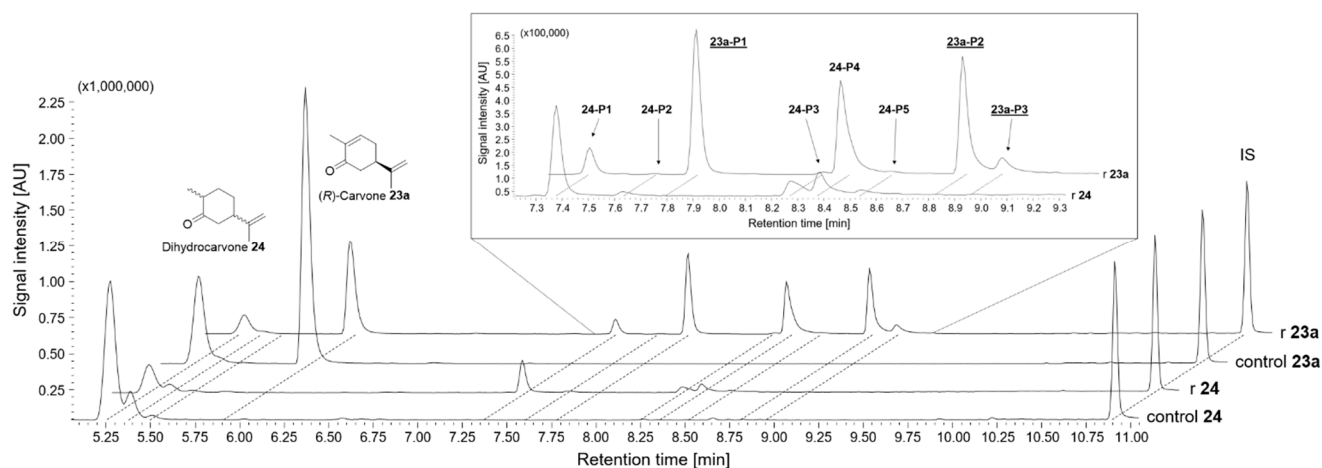


**Figure 4.** Comparison of GC/MS chromatograms of (R)-(-)-carvone **23a** and dihydrocarvone **24** conversion. Conversions with rCYP4B1 (r) and a reaction without P450 (control) are shown as examples. IS = internal standard. The inset depicts the products formed by rCYP4B1 from **23a** and **24**; the three products formed solely from **23a** are underlined.

From group V, (R)-(+)- $\alpha$ -pinene **26a** was the only compound for which conversion was observed.  $\alpha$ -Pinene **26** is a compound found in several types of wood (e.g., pines and cedars) and is volatile under standard conditions. Its concentrations in the air can reach up to  $150 \text{ mg m}^{-3}$  in wood-processing workplaces [44,45], making it worthwhile to study the metabolism in the respiratory tract where CYP4B1 is expressed. In our screening, the conversion rates of (R)-(+)- $\alpha$ -pinene **26a** reached 34% and 30% using rCYP4B1 and chCYP4B1, respectively, but only 9% with mlCYP4B1. Interestingly, (S)-(-)- $\alpha$ -pinene **26b** was not converted by any ortholog. For **26a**, myrtenol **26a-P1** was the only product observed. The other products found, namely verbenol, verbenone, and 2,3-epoxy pinene, are most likely formed by non-enzymatic autoxidative processes, since they were also present in the negative control without CYP4B1. Myrtenol **26a-P1** was also found as a urinary metabolite of  $\alpha$ -pinene **26** in rabbits [46]. In conjunction with our results, this suggests that rCYP4B1 might also be involved in the metabolic processing of  $\alpha$ -pinene **26a**. In a later study, an in vivo test in humans after oral admission was carried out in which myrtenol **26a-P1** and *cis*- and *trans*-verbenol were likewise identified in blood and urine samples [47]. This observation showed that other P450s must also be involved in the metabolism of  $\alpha$ -pinene **26**, since the native form of human CYP4B1 is catalytically inactive and therefore cannot be responsible for these conversion products.

#### 2.3.4. Group VI: Aromatic Hydrocarbons

Aromatic hydrocarbons are organic compounds commonly found in petroleum products such as plastics, paints, and adhesives, as well as their fumes during combustion. Other sources that release them into the environment include tobacco smoke and traffic exhaust fumes, as well as the burning of natural materials such as wood and coal [48–52]. Thus, they are widespread compounds, which are frequently absorbed via the respiratory tract and are typically metabolized by CYP1A1, CYP1B1, or CYP1A2 [48,52,53].

Group VI contained cumene **31**, styrene **32**, naphthalene **33**, thioanisole **34**, 2-aminoanthracene (2-AA) **36**, and the known CYP4B1 substrate 2-aminofluorene (2-AF) **35** [23]. Remarkably, conversion was observed for all orthologs with all compounds, except 2-AA **36**. This resulted in hydroxylated or epoxidized products, and in the case of thioanisole **34** in S-oxidation, a reaction type that to our knowledge had so far not been described for CYP4B1.

The highest conversion was observed for cumene **31** (62% for rCYP4B1; 30% and 37% with chCYP4B1 and mlCYP4B1, respectively). Cumene **31** was hydroxylated at its propyl group, forming 2-phenyl-1-propanol **31-P1** (36–64% ee (*S*)) as a product, which is further oxidized to the respective aldehyde **31-P2** (Figure 5A). Product **31-P1** was previously described by Chen et al., who analyzed the lung tissue of mice and rats [54]. They associated it with hydroxylation by CYP2F1 or CYP2F2, which are both also described as being predominantly expressed in lung tissues. Our *in vitro* results, as well as previous results published by Henne et al. using recombinant rCYP4B1 [55], suggest that CYP4B1 may also play a role in the metabolism of cumene **31** in the lung, at least in rabbits, green monkeys, and mouse lemurs.

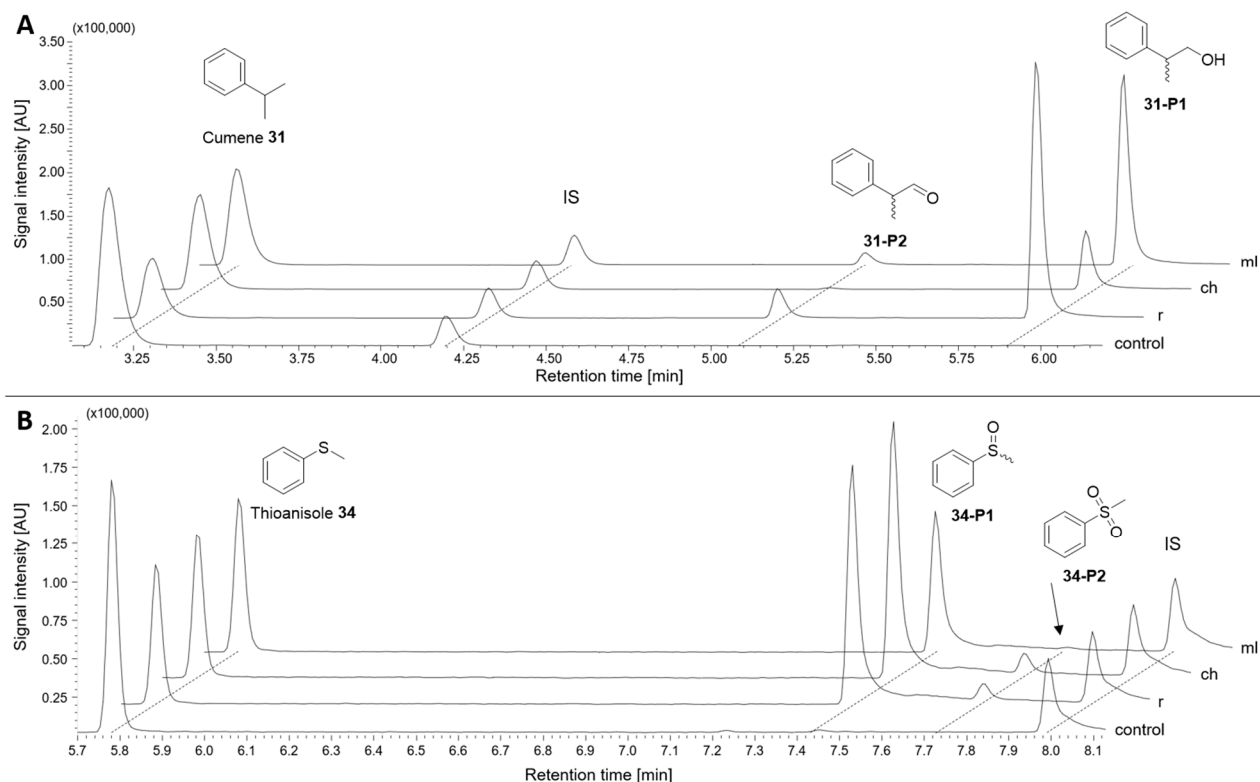


**Figure 5.** GC/MS chromatograms of cumene **31** and thioanisole **34** conversion. Comparison between rCYP4B1 (r), chCYP4B1 (ch), mlCYP4B1 (ml), and a reaction without P450 (control). Substrates and identified products are pointed out; IS: internal standard; (A) cumene **31** with **31-P1** and **31-P2** as products; (B) thioanisole **34** with **34-P1** and **34-P2** as products.

Thioanisole **34** conversions of 50% (rCYP4B1), 57% (chCYP4B1) and 43% (mlCYP4B1) were determined, with sulfoxide **34-P1** and sulfone **34-P2** as reaction products (Figure 5B). All three orthologs showed a preference towards reacting to the *R*-sulfoxide (*er* = ~75:25). This reaction contributes to detoxification by making the products more polar and therefore more water-soluble, thus being easier to excrete via the urine. To the best of our knowledge, there are no publications so far reporting that thioanisole **34** can be converted by mammalian P450s. However, this reaction has previously been described for bacterial P450s, such as CYP102A1 (BM3), CYP116B4, and P450<sub>cam</sub>, as well as unspecific peroxygenase (UPO) and P450 peroxygenases, such as *Aae*UPO or CYP119 [56–59]. P450<sub>cam</sub> catalyzes the sulfoxidation of thioanisole **34** with turnover rates of 3.5 nmol<sub>thioanisole</sub>/nmol<sub>P450</sub>/min [60], which is similar to those of CYP4B1 (3.8–4.4; calculated from the conversions summarized in Section 2.3.9). These results highlight the importance of further investigation of animal P450s in the detoxification of environmental toxins.

Styrene **32** and naphthalene **33** are well-known lung toxicants with potential carcinogenic effects [61–64]. All three tested CYP4B1 orthologs catalyzed the regioselective bioactivation of styrene **32**, forming 7,8-styrene epoxide **32-P1** with no clear stereochemical preference (9–14 % ee (*S*)) as the only P450 product, which is capable of forming carcinogenic DNA-adducts [65]. In addition, 2-phenylethan-1-ol **32-P1\*** was present in all samples (Figure 6A), which may have been the result of hydrogenation of the epoxide by endogenous *E. coli* proteins. That reaction is also described in humans as a detoxification step by microsomal epoxide hydrolases [66,67]. Other lung P450s, such as CYP2E1, CYP2F1, and CYP2F2, are also known to be involved in the metabolism of styrene **32**, leading to **32-P1** [68,69]. Naphthalene **33** conversions led to two hydroxylated products, namely 1-naphthol **33-P1** and 2-naphthol **33-P2**. With rCYP4B1 and chCYP4B1 1-naphthol **33-P1** was the main product with around 83%, while mlCYP4B produced both products in almost equal amounts (53%/47%; Figure 6B). These products were also described for P450BM3 variants, such as A74G/F87V/L188Q, where mainly 1-naphthol (96%) was formed [70]. Notably, the reactive epoxide metabolite of naphthalene **33**, which is described for its conversion by CYP2F [71], was not detected with CYP4B1, indicating that CYP4B1 takes part in detoxification of naphthalene **33** rather than its activation.

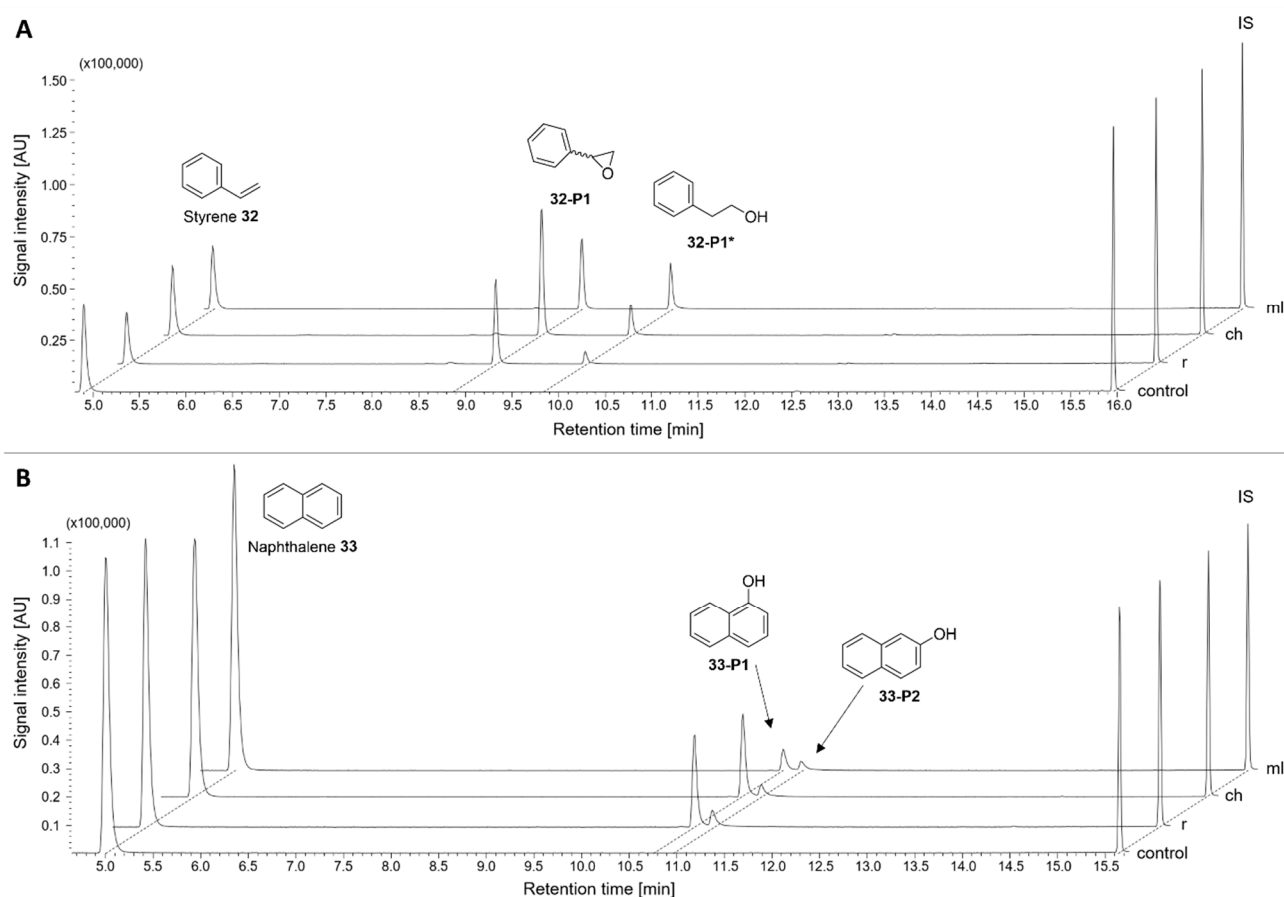


**Figure 6.** GC/MS chromatograms of styrene **32** and naphthalene **33** conversion. Comparison between rCYP4B1 (r), chCYP4B1 (ch), mlCYP4B1 (ml), and a reaction without P450 (control). Substrates and identified products are pointed out; IS: internal standard; (A) styrene **32** with **32-P1** as product and **32-P1\*** as non-P450 catalyzed byproduct; (B) naphthalene **33** with **33-P1** and **33-P2** as products.

Of the two cyclic aromatic amines 2-AF **35** and 2-AA **36** tested here, only 2-AF **35** led to hydroxylated products by all three orthologs with conversions between 26% (mlCYP4B1) and 45% (rCYP4B1). No conversion could be observed with 2-AA **36**. Testing of 2-AF **35** in former studies with cell survival assays of HepG2-cells expressing rCYP4B1 revealed

unspecific cytotoxic effects in higher substrate concentrations, which may be explained by the production of non-toxic metabolites [23].

### 2.3.5. Group VII: Heterocycles

Furan-containing heterocyclic compounds are well-known pro-toxic substrates for CYP4B1, in particular rCYP4B1 [23], with 4-ipomeanol (4-IPO) **37** as its so-called 'hallmark-substrate' [16,24,27,72,73]. In previous studies, we confirmed them as substrates for rCYP4B1. Here, we compared the results for rCYP4B1 with those of the two primate orthologs. rCYP4B1 had the highest activity against 4-IPO **37** (51%), while the primate orthologs showed conversions of 26% and 31%. Perilla ketone (PK) **38** differs from 4-IPO **37** only by a methyl group instead of a hydroxy group at the end of the alkyl chain. However, this led to complete conversion (>99%) with all three orthologs under the 'standard' reaction setup (200  $\mu$ M, 90 min), so that a second experiment was conducted in order to recognize differences in activities between the orthologs (300  $\mu$ M, 30 min). Under these conditions, ~93% conversion was determined for chCYP4B1 and mlCYP4B1, while rCYP4B1 achieved 'only' 81%. The preference for PK **38** over 4-IPO **37** of rCYP4B1 was also observed by Roellecke et al. and was attributed to the fact that, unlike 4-IPO **37**, PK **38** can also be hydroxylated at its alkyl chain in addition to forming the reactive species by epoxidation of the furan ring [23]. The observation that the primate orthologs have a ~threefold higher activity towards PK **38** in comparison to 4-IPO **37** therefore indicates an even higher preference for alkyl chain hydroxylation, as also observed with fatty acids (compare Figure 3).

Indole **39** is a heterocyclic amine found in essential oils of jasmine and flowers, as well as a breakdown product of tryptophan in feces. It is a known substrate of several animal P450s, such as CYP2A6 and CYP2C19, where 3-hydroxyindole and indoxyl are the major metabolites [74]. By conversion with CYP4B1, only one product was detected and identified as indoline-2-one **39-P1**. This metabolite is discussed as producing a toxic effect upon mammalian tissues and having an inhibitory effect on the central nervous system [75–77].

The association of 3-methylindole (3-MI) **40** with CYP4B1 has previously been described in the literature [23]. 3-MI **40** is a fermentation product of tryptophan from rumen and intestinal microbes and is also found in cigarette smoke [78,79]. It is reported to be a pro-toxic compound with a methylene imine as the toxic product formed by initial dehydrogenation reaction with several pulmonary P450s, including CYP4B1 [79–81]. Lung-specific toxicity in vivo was observed first in several animals such as cattle and rabbits [82]. Later, the reaction with rCYP4B1 and its toxicity in in vitro studies could be confirmed [23]. Here, it is confirmed that 3-MI **40** is also converted by chCYP4B1 (47%) and mlCYP4B1 (albeit only 18%).

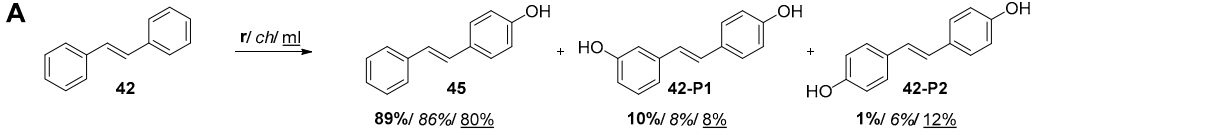
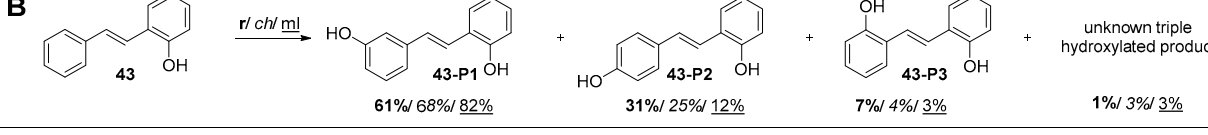
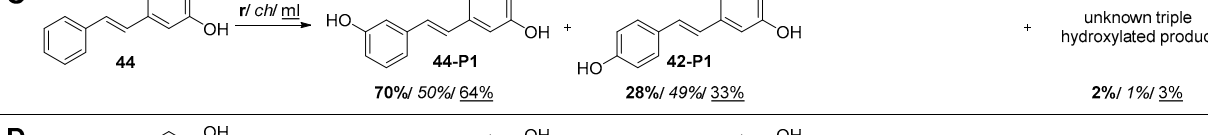
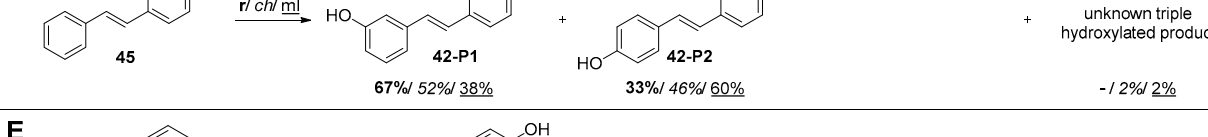
Myristicin **41** is a naturally occurring heterocyclic benzodioxole derivative found in several herbs and spices, most notably nutmeg. It is known for its biological activities such as antimicrobial, insecticidal, or anti-inflammatory activity, as well as being a psychoactive drug in higher doses, which has led to medicinal interest, but also concerns about potential toxicity [83–85]. The toxicity of myristicin **41** may be due to activation by P450s forming 1'-hydroxymyristicin, which has been described for several hepatic P450s including CYP1A1 and CYP2C9 [86]. Another metabolite from **41** is 5-allyl-1-methoxy-2,3-dihydroxybenzene (6-hydroxyeugenol) **41-P1**, which has been described as resulting from demethylation by CYP1A2 and CYP3A4 [87]. Here, it was found that all three CYP4B1 orthologs are also capable of performing this ring-opening O-demethylation reaction. Although this reaction product has not shown direct toxic effects in previous studies, it might still be converted to

its toxic form by other enzymes via 1'-hydroxylation on the allylic side chain, as has been shown for methyl eugenol, which shares the same allylic group [84,88].

### 2.3.6. Group VIII: Stilbene and Stilbenoids

Stilbene and stilbenoids are a class of naturally occurring compounds found in a variety of plants, including grapes, berries, nuts, and certain types of wood, such as pine and eucalyptus [89]. They have attracted the attention of the scientific community for their potential health benefits, comprising potential cancer prevention and treatment, with resveratrol **47** being the most extensively studied [90–92]. They can exist in two configurational isomers: *trans*-stilbene **42** (*E*-stilbene) and *cis*-stilbene (*Z*-stilbene), with the *trans* form being more abundant and stable in nature [90]. Therefore, our screening focused only on the *trans*-isomers. With respect to P450s, stilbenoids can act either as inhibitors or as substrates. For example, resveratrol **47** has been described as an inhibitor of CYP1A1 and CYP3A4, while the former also catalyzes the biotransformation of *trans*-stilbene **42** to *trans*-4-hydroxystilbene **45** in rats and humans [93,94].

Here, *trans*-stilbene **42** and monohydroxylated *trans*-stilbenoids **43–45** were identified as substrates for the three CYP4B1 orthologs, with mCYP4B1 showing the highest activity (87% conversion of *trans*-stilbene **42**). In all cases, hydroxylations at positions 4, 4', and 3' were favored, and thus 4-hydroxystilbene **45**, 4,4'-dihydroxystilbene **42-P2**, and 4,3'-dihydroxystilbene **42-P1** were formed from *trans*-stilbene **42** (Figure 7).

<b>A</b>		<p><b>45</b>: 89%/<b>86%</b>/<u>80%</u></p> <p><b>42-P1</b>: 10%/8%/8%</p> <p><b>42-P2</b>: 1%/6%/12%</p>
<b>B</b>		<p><b>43-P1</b>: 61%/<b>68%</b>/<u>82%</u></p> <p><b>43-P2</b>: 31%/25%/12%</p> <p><b>43-P3</b>: 7%/4%/3%</p> <p>unknown triple hydroxylated product: 1%/3%/3%</p>
<b>C</b>		<p><b>44-P1</b>: 70%/<b>50%</b>/<u>64%</u></p> <p><b>42-P1</b>: 28%/49%/33%</p> <p>unknown triple hydroxylated product: 2%/1%/3%</p>
<b>D</b>		<p><b>42-P1</b>: 67%/<b>52%</b>/<u>38%</u></p> <p><b>42-P2</b>: 33%/46%/60%</p> <p>unknown triple hydroxylated product: -/2%/2%</p>
<b>E</b>		<p><b>47</b>: 91%/<b>93%</b>/<u>92%</u></p> <p>unknown triple hydroxylated product: 9%/7%/8%</p>

**Figure 7.** Product distribution of in vitro reactions with *trans*-stilbene **42** and stilbenoids **43–46**. Reactions with (A) *trans*-stilbene **42**; (B) *trans*-2-hydroxystilbene **43**; (C) *trans*-3-hydroxystilbene **44**; (D) *trans*-4-hydroxystilbene **45** and (E) pinosylvin **46** as substrates. Ortholog specific product distribution is shown in %; rCYP4B1 in bold, chCYP4B1 in italic, mCYP4B1 underlined.

In the case of mono-hydroxylated stilbenes **43**, **44**, or **45** as substrates, the 3'-position was preferred for the second hydroxylation (**43-P1**, **44-P2**, **42-P1**), followed by the 4'-position (**43-P2**, **44-P1**, **42-P2**). Only in the case of 2-hydroxystilbene **43** was the 2'-position also addressed to a small extent, resulting in **43-P3**. In no case could a second hydroxylation on the same ring be detected.

Several studies have shown that not only resveratrol **47**, but also dihydroxystilbenes such as 4,4'-hydroxystilbene **42-P2** have high potential as anticancer agents by, for example, inhibiting the proliferation of human breast cancer cells, preventing colon tumor growth, or suppressing metastatic colonization in the lungs [91,95,96]. Since the natural occurrence of these dihydroxystilbenes is limited, such as 4,4'-dihydroxystilbene **42-P2**, which is mainly described as a minor secondary metabolite produced by *Yucca periculosa* [97], the biocatalytic production of 4,4'-dihydroxystilbene **42-P2** from stilbene **42** and 4-hydroxystilbene **45** is of interest.

### 2.3.7. Group IX: Vanilloids

Vanilloids, for example capsaicin **48** and gingerol **49**, are a diverse group of compounds characterized by their ability to interact with the transient receptor potential vanilloid 1 (TRPV1) receptor, sharing structural similarities, for example a phenol fragment and an alkyl chain [98–100]. While piperine **50** does not possess this characteristic vanillyl group, it can be classified as a vanilloid-like substance in the context of its interaction with the TRPV1 receptor [101,102]. These compounds are found in various plants, such as chili peppers, black pepper, and ginger, and exhibit a wide range of biological activities, including analgesic, anti-inflammatory, and antioxidant properties. The conversion by P450s produces various metabolites, including electrophilic products and radicals, which are likely to cause their biological effects and potential toxicity, which has been described previously [103–105]. Capsaicin **48** is also used as a treatment for allergic and non-allergic rhinitis in aerosols, and therefore potentially interacts with pulmonary enzymes [106,107].

Remarkably, conversion of the chosen vanilloids was only observed with the two primate orthologs, but (almost) not with rCYP4B1, which is supported by the observation that in the initial screening a spectral shift (type I) was only observed with mCYP4B1, but not with rCYP4B1. Gingerol **49** was best accepted (70% and 51% conversion by chCYP4B1 and mCYP4B1, respectively), whereas piperine **50** was only converted to a small extent (2% max.). Reactions with capsaicin **48** and gingerol **49** resulted in terminal hydroxylation at the alkyl chain, but not at the vanillyl group (Figure 8), as confirmed by LC/MS/MS analysis, where the dissociated vanillyl group of the reaction products (**48-P1**, **49-P1**) has the same  $m/z$  value as the respective substrates (Figure 8B). The orientation of capsaicin **48** as obtained from the docking results also indicates hydroxylation at the terminus of the carbon chain, in agreement with the experimental results (Figure 8C).

The same reaction on gingerol **49** is also described for human CYP2C19 and CYP1A2, while both also catalyze oxidations, as well as demethylation reactions at the vanillyl group [108]. Terminal and subterminal hydroxylation of the alkyl chain of capsaicin **48** is known for hepatic P450s, such as CYP2E1 and CYP2C9, but was not detected for goat CYP4B1 in the same study [109]. However, CYP2E1 is also expressed in the lung and shares styrene **32** activity with CYP4B1 (see Section 2.3.4). The binding mechanism of capsaicin **48** in CYP2C9 has been hypothesized to be similar to that of fatty acids and *n*-alkanols in CYP4B1 by stabilization of the 'head group' via amino acids on the opposite side of the heme in the narrow active center, leading to terminal hydroxylation of the alkyl chain [14,104].

Other human P450s, such as CYP1A2, CYP2C19, and CYP2B6, catalyze the bioactivation of capsaicin **48** and its derivatives by, for example, O-demethylation and aromatic hydroxylation, to form toxic electrophilic metabolites [103,104,110]. These reaction products were not detected in our experimental setup, suggesting that CYP4B1 is not involved in the bioactivation, but rather in detoxification of capsaicin **48**. However, according to our results, this only applies to the two primate orthologs, but not to rabbits and, according to

previous studies, also not to goats, as no reaction on capsaicin **48** could be detected [109]. These results highlight again the importance of investigating species differences of CYP4B1.

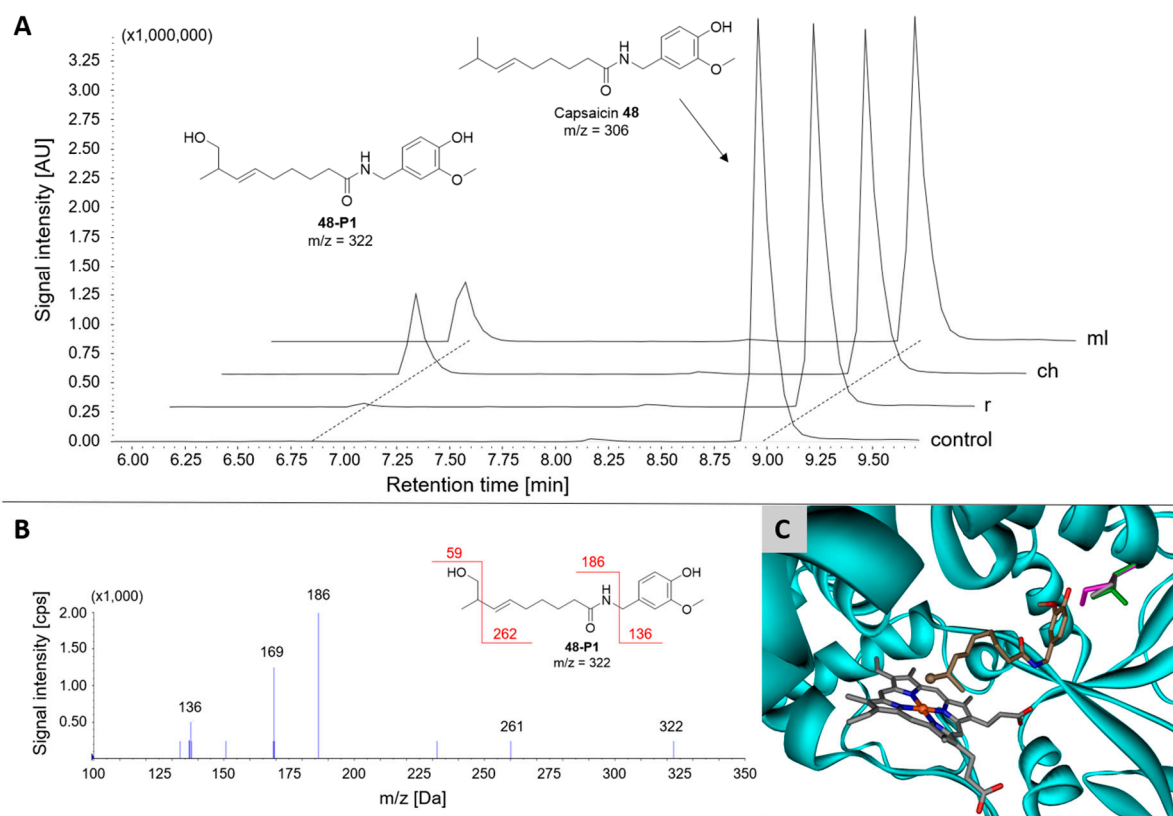


**Figure 8.** Identification of capsaicin metabolite **48-P1**. **(A)** LC/ESI-MS chromatograms of *in vitro* conversions with rCYP4B1 (r), chCYP4B1 (ch), and mlCYP4B1 (ml) in comparison to a reaction without P450 (control); substrate capsaicin **48** and its product **48-P1** are pointed out; **(B)** identification of **48-P1** via MS/MS fragmentation suggests terminal hydroxylation; **(C)** overlay of the crystal structure of rCYP4B1 (5T6Q.pdb) with the homology models of chCYP4B1 and mlCYP4B1 with docked capsaicin **48** shown in light brown with the hydroxylated position depicted as a sphere. The residues of the binding pocket differ only in position 221: grey: rCYP4B1, green: chCYP4B1, mauve: mlCYP4B1. Some parts of the protein have been omitted for clarity.

### 2.3.8. Group X: Miscellaneous

Group X is a miscellaneous group containing all compounds that did not fit into groups I–IX and includes flavones, isoflavones, flavonoids, and steroids. They are naturally occurring substances that have been described as substrates for several human P450s such as CYP1A1, CYP1A2, and CYP1B1 [111,112]. This group was included since isoflavones and flavonoids repeatedly induced spectral changes in the initial screening of the natural product library and therefore initially appeared to be promising candidates for CYP4B1.

Unexpectedly, for most of the tested compounds no or only very small amounts of products were observed during the *in vitro* experiments, even after prolonged incubation for 24 h (<1%; oxidation sites could not be identified due to low quantities).

The only exception was the isoflavone genistein **52**, for which a maximum conversion of 11% was observed by rCYP4B1 after 24 h incubation. Structurally related natural products, such as apigenin **51** and kaempferol **53**, showed a maximum conversion of only ~1%. Since members of these substance groups are also known as inhibitors of other animal P450s, for example apigenin **51**, kaempferol **53**, and quercetin **54** for CYP3A4, and genistein **52** for CYP1A2 and CYP1B1, they may also have inhibitory effects on CYP4B1 activity which led to the observed spectral changes [113–115].

None of the orthologs showed any activity with cholecalciferol **59** or testosterone **60**. Considering the results with FAs (Figure 2; C16-FA **8**) and acyclic terpenoids (no conversion with farnesol and derivatives **19–21**; Section 2.3.2), it is suggested that these compounds are either too large to be accommodated in the binding pocket, or are likely to be inhibitors rather than substrates, as indicated by their predicted unusually high binding affinities from in silico docking (e.g., <100 nM for cholecalciferol and <30 nM for testosterone).

### 2.3.9. Summary and Overview of Substrate Conversion by CYP4B1

All results obtained from the in vitro conversions with rCYP4B1, chCYP4B1, and mlCYP4B1 are summarized in Table 1, including the conversion and the respective main products that were identified by either GC/MS, LC/MS, or LC/MS/MS analysis.

**Table 1.** Overview of substrate conversion by rCYP4B1, chCYP4B1, and mlCYP4B1 within the systematic compound library. The mean conversion  $\pm$  standard deviation (SD; for conversions > 5%) of at least three independent experiments after in vitro conversion with 200  $\mu$ M substrate in 90 min is shown. \* = mixture of stereoisomers; <sup>a</sup> = 200  $\mu$ M substrate, 24 h conversion; <sup>b</sup> = 300  $\mu$ M substrate, 30 min conversion; <sup>c</sup> = hydroxylation(s)/epoxidation(s) at unknown position(s); <sup>d</sup> = product identification based on literature data [23,27,79].

No	Substance Group	Compound	Conversion [%]			Main Product(s) Observed
			r	ch	mL	
1	I Saturated fatty acid	Nonanoic acid	14 $\pm$ 6	12 $\pm$ 1	6 $\pm$ <1	$\omega$ -, $\omega$ -1-OH
2		Decanoic acid	46 $\pm$ 3	19 $\pm$ 2	11 $\pm$ <1	$\omega$ -, $\omega$ -1-OH
3		Undecanoic acid	52 $\pm$ 3	39 $\pm$ 10	38 $\pm$ 6	$\omega$ -, $\omega$ -1-OH
4		Dodecanoic acid	50 $\pm$ 1	85 $\pm$ 2	85 $\pm$ 1	$\omega$ -, $\omega$ -1-OH
5		Tridecanoic acid	9 $\pm$ 1	78 $\pm$ 1	67 $\pm$ 7	$\omega$ -, $\omega$ -1-OH
6		Tetradecanoic acid	5	48 $\pm$ 3	32 $\pm$ 3	$\omega$ -, $\omega$ -1-OH
7		Pentadecanoic acid	1	5	2	$\omega$ -, $\omega$ -1-OH
8		Hexadecanoic acid	-	1	1	$\omega$ -, $\omega$ -1-OH
9	II Fatty alcohol ( <i>n</i> -alkanol)	1-Decanol	10 $\pm$ 2	11 $\pm$ 2	9 $\pm$ <1	$\omega$ -OH
10		1-Dodecanol	18 $\pm$ 1	9 $\pm$ 1	16 $\pm$ 1	$\omega$ -, $\omega$ -1-OH
11		1-Tetradecanol	5	15 $\pm$ 4	18 $\pm$ 1	$\omega$ -1-OH, $\omega$ -OH, $\omega$ -2-OH
12		1-Hexadecanol	5	15 $\pm$ 2	13 $\pm$ 1	$\omega$ -OH
13	III Acyclic terpenoid	Geraniol	61 $\pm$ 3	69 $\pm$ 2	54 $\pm$ 3	8-Hydroxygeraniol <b>13-P1</b>
14		Geranyl acetate	24 $\pm$ 1	49 $\pm$ 7	44 $\pm$ 6	Epoxides <sup>c</sup>
15		Geranyl acetone	24 $\pm$ 1	51 $\pm$ 2	38 $\pm$ 4	Epoxides <sup>c</sup>
16		Nerol	15 $\pm$ 2	13 $\pm$ 1	6 $\pm$ 1	8-Hydroxynerol <b>16-P1</b>
17		Neryl acetate	10 $\pm$ 1	42 $\pm$ 4	14 $\pm$ 1	Epoxides <sup>c</sup>
18		Neryl acetone	8 $\pm$ <1	16 $\pm$ 1	8 $\pm$ 2	Epoxides <sup>c</sup>
19		Farnesol *	-	-	-	
20		Farnesyl acetate *	-	-	-	
21		Farnesyl acetone *	-	-	-	
22a/b	IV	Limonene ( <i>R/S</i> )	-/-	-/-	-/-	
23a/b	Monocyclic terpene/terpenoid	Carvone ( <i>R/S</i> )	73 $\pm$ 2/ 44 $\pm$ 2	50 $\pm$ 3/ 29 $\pm$ 1	29 $\pm$ 2/ 25 $\pm$ 2	n.d. <sup>c</sup>
24		Dihydrocarvone * (mixture of isomers)	62 $\pm$ 2	44 $\pm$ 2	29 $\pm$ 2	n.d. <sup>c</sup>
25		Eugenol	-	-	-	
26a/b	V	$\alpha$ -Pinene ( <i>R/S</i> )	34 $\pm$ 1/-	30 $\pm$ 1/-	9 $\pm$ 2/-	Myrtenol <b>26a-P1</b>
27	Bicyclic terpene/terpenoid	Camphor	-	-	-	
28		Valencene	-	-	-	
29		Nootkatone	-	-	-	
30		Coumarin	-	-	-	

Table 1. Cont.

No	Substance Group	Compound	Conversion [%]			Main Product(s) Observed		
			r	ch	mL			
31	VI	Cumene	62 ± 5	30 ± <1	37 ± 8	2-Phenyl-1-propanol <b>31-P1</b>		
32			56 ± 6% ee (S)	64 ± 2% ee (S)	36 ± 8% ee (S)			
33		Styrene	25 ± 4	36 ± 2	24 ± 1	7,8-Styrene epoxide <b>32-P1</b>		
34			11 ± 4% ee (S)	9 ± 3% ee (S)	15 ± 5% ee (S)			
35		Aromatic hydrocarbon	Naphthalene	23 ± 2	22 ± 3	12 ± 3	1-/2-Naphthol <b>33-P1/33-P2</b>	
36			Thioanisole	50 ± 5	57 ± 9	43 ± 6		
37	VII	2-Aminofluorene	46 ± 3% ee (R)	49 ± 1% ee (R)	53 ± 2% ee (R)	Sulfoxide <b>34-P1</b> , sulfone <b>34-P2</b>		
38		2-Aminoanthracene	45 ± 2	39 ± 3	26 ± 10			
39		4-Ipomeanol	-	-	-		n.d. <sup>c</sup>	
40		Heterocycle	Perilla ketone <sup>b</sup>	51 ± 6	26 ± 4		33 ± 2	Furan epoxide <sup>d</sup>
41			Indole	81 ± 3	92 ± 2		94 ± 2	Furan epoxide <sup>d</sup>
42	VIII	3-Methylindole	46 ± 2	65 ± 1	18 ± <1	Indoline-2-one <b>39-P1</b>		
43		Myristicin <sup>a</sup>	38 ± 8	47 ± 4	18 ± 7	3-Methyleneindolenine <sup>d</sup>		
44			52 ± 2	38 ± 2	28 ± 1			
45		Stilbene/ stilbenoid	<i>trans</i> -Stilbene	27 ± 3	77 ± 3	87 ± 3	4-OH <b>45</b> , 3,4'-OH <b>42-P1</b> , 4,4'-OH <b>42-P2</b>	
46			<i>trans</i> -2-Hydroxystilbene	40 ± 5	77 ± 5	47 ± 6	2,3'-OH <b>43-P1</b> , 2,4'-OH <b>43-P2</b> , 2,2'-OH <b>43-P3</b>	
47			<i>trans</i> -3-Hydroxystilbene	14 ± 1	26 ± 1	36 ± 5	3,3'-OH <b>44-P1</b> , 3,4'-OH <b>42-P1</b>	
48	IX	<i>trans</i> -4-Hydroxystilbene	5 ± 1	30 ± 4	31 ± 5	3,4'-OH <b>42-P1</b> , 4,4'-OH <b>42-P2</b>		
49		Pinosylvin	6 ± 1	2	<1	Resveratrol <b>47</b>		
50		Resveratrol	-	-	-			
51	X	Capsaicin	1	17 ± 2	16 ± 1	17-Hydroxycapsaicin <b>48-P1</b>		
52		Vanilloid	[6]-Gingerol	0	70 ± <1	51 ± 4	10-Hydroxy-[6]-gingerol 49-P1	
53			Piperine <sup>a</sup>	<1	2	1	n.d. <sup>c</sup>	
54		Miscellaneous	Apigenin <sup>a</sup>	<1	<1	<1	n.d. <sup>c</sup>	
55			Genistein <sup>a</sup>	11 ± 5	5	2	n.d. <sup>c</sup>	
56			Kaempferol <sup>a</sup>	<1	<1	<1	n.d. <sup>c</sup>	
57			Quercetin <sup>a</sup>	-	-	-		
58			Flavone <sup>a</sup>	-	-	-		
59			7-Hydroxyflavone <sup>a</sup>	3	2	1	n.d. <sup>c</sup>	
60		5-,7- Dihydroxyflavone <sup>a</sup>	<1	<1	<1	n.d. <sup>c</sup>		
61	6-,7- Dihydroxyflavone <sup>a</sup>	-	-	-				
62	Cholecalciferol <sup>a</sup>	-	-	-				
63	Testosterone <sup>a</sup>	-	-	-				

### 3. Materials and Methods

#### 3.1. Plasmid Construction for *cyp4b1* Expression in *E. coli*

*cyp4b1*-genes (chCYP4B1, *Chlorocebus sabaeus*, XM007978860.2; mCYP4B1, *Microcebus murinus*, XM\_012776101.1; human codon-optimized synthetic genes obtained from Genearth AG, Regensburg, Germany) were amplified via PCR and ligated into plasmid pET22b(+) as described previously for rCYP4B1 [23]. To achieve soluble expression, the N-terminal membrane anchors were removed by truncation of amino acids 2 to 24 (N<sub>Δ2-24</sub>) and alanine was added as the second amino acid. For ligation into pET22b(+), the restriction sites

NdeI and NotI were utilized, supplying the amino acid sequence AAALHHHHHHH to the C-terminus of CYP4B1; the 6× His tag was utilized for IMAC purification.

### 3.2. Protein Expression in *E. coli* and Purification of Recombinant Enzymes

#### 3.2.1. CYP4B1 Orthologs

Strain *E. coli* OverExpress C43(DE3) [ $F^- ompT hsdS_B (r_B^- m_B^-) gal dcm$  (DE3)] (Lucigen Corporation, Middleton, WI, USA) was used for *cyp4b1* expression. Main cultures in 2 L shake flasks containing 400 mL terrific broth medium supplemented with 100  $\mu\text{g mL}^{-1}$  ampicillin and 400  $\mu\text{L}$  trace element solution (27  $\text{g L}^{-1}$   $\text{FeCl}_3 \cdot 6\text{H}_2\text{O}$ , 2  $\text{g L}^{-1}$   $\text{ZnCl}_2 \cdot 4\text{H}_2\text{O}$ , 2  $\text{g L}^{-1}$   $\text{CoCl}_2 \cdot 6\text{H}_2\text{O}$ , 2  $\text{g L}^{-1}$   $\text{Na}_2\text{MoO}_4 \cdot 2\text{H}_2\text{O}$ , 2  $\text{g L}^{-1}$   $\text{CaCl}_2 \cdot 2\text{H}_2\text{O}$ , 1  $\text{g L}^{-1}$   $\text{CuCl}_2$ , 0.5  $\text{g L}^{-1}$   $\text{H}_3\text{BO}_3$ , 100  $\text{mL L}^{-1}$  37% HCl) were grown at 37 °C, 180 rpm. Expression was induced at  $\text{OD}_{600} = 0.6$  with 0.5 mM isopropyl  $\beta$ -D-1-thiogalactopyranoside (IPTG). At the same time, 0.5  $\mu\text{M}$   $\delta$ -aminolevulinic acid was added and the culture conditions set to 27 °C, 120 rpm for 48 h.

Cells were harvested by centrifugation (5000×  $g$ , 30 min, 4 °C; Avanti J-26 XP, Beckman Coulter, Brea, CA, USA) and the obtained cell pellet was resuspended in a 50 mM potassium phosphate buffer (KPi), pH 7.4, containing 20% glycerol and 500 mM KCl. The cell suspension was supplemented with 0.5% ( $v/v$ ) of a solution of 'cComplete™ EDTA-free protease inhibitor cocktail tablets' prepared according to the manufacturer's manual (Roche Diagnostics, Mannheim, Germany), 100  $\mu\text{M}$  C12-FA from a 100 mM stock solution in dimethyl sulfoxide (DMSO), 20 mM  $\beta$ -mercaptoethanol, 5 mM imidazole, and 1% ( $w/v$ ) sodium cholate. Cell disruption was performed by sonification (15 min, 15 s intervals with 15 s breaks; Sonifier SFX 550, Branson Ultrasonic, Brookfield, CT, USA). The insoluble proteins and cell debris were removed by ultracentrifugation (150,000×  $g$ , 1 h, 4 °C; Optima XPN-80, Beckman Coulter, Brea, CA, USA).

For purification by affinity chromatography (IMAC), the soluble protein fraction was incubated with 6 mL nickel nitrilotriacetic acid-agarose (Ni-NTA-Superflow, Cytiva, Marlborough, MA, USA) that was equilibrated with buffer (50 mM KPi, pH 7.4, 20% glycerol, 500 mM KCl, 5 mM imidazole, 0.2% ( $w/v$ ) sodium cholate) for 30 min at 10 °C under gentle mixing in an overhead shaker. The suspension was then poured into a gravity column, the flow-through was discarded, and the resin was washed with five column volumes of wash buffer (50 mM KPi, pH 7.4, 20% glycerol, 40 mM imidazole, 0.2% ( $w/v$ ) sodium cholate). Bound CYP4B1 was eluted with elution buffer (500 mM imidazole in wash buffer) and concentrated by ultrafiltration (30 kDa molecular weight cut-off; 4000×  $g$ , 4 °C, Allegra X-15R, Beckman Coulter, Brea, CA, USA). Desalting and removal of detergent and imidazole were performed by application of a PD MidiTrap G-25 column (Cytiva, Marlborough, MA, USA) that was equilibrated with storage buffer (100 mM KPi, pH 7.4, 20% glycerol, 0.1 mM EDTA). CYP4B1 concentrations and yield were calculated from CO-difference spectra with  $\epsilon_{450-490} = 91 \text{ mM}^{-1} \text{ cm}^{-1}$  [116] (Supplementary Figure S1 and Supplementary Table S6). Purified enzymes were stored at −20 °C until further use.

#### 3.2.2. Fdr and YkuN

Expression and purification of flavodoxin (YkuN) from *Bacillus subtilis* and flavodoxin reductase (Fdr) from *E. coli* JM109 were carried out as described previously [117].

#### 3.2.3. bCYB5

For expression of bovine cytochrome  $b_5$  (bCYB5), plasmid pET17b (kindly provided by Prof. Rita Bernhardt (as described in [118])) was utilized in *E. coli* OverExpress C43(DE3) following an expression protocol described by Mulrooney et al. [119]. Purification via IMAC was carried out following the protocol described for bovine CPR by Zöllner et al. [120].

### 3.2.4. GDH

Glucose dehydrogenase (GDH) from *Bacillus megaterium* (gdhIV; GenBank D10626) was expressed in *E. coli* BL21(DE3) from pET22b(+) and partially purified by a combination of salt precipitation and heat denaturation of endogenous *E. coli* proteins as described elsewhere [121].

### 3.3. Reconstitution of CYP4B1 Activity for Substrate Screening

Substrate conversion was carried out in 50 mM  $KP_i$ , pH 7.5, in a total volume of 100  $\mu$ L. Reaction mixtures contained 0.25  $\mu$ M CYP4B1, 2  $\mu$ M Fdr, 20  $\mu$ M YkuN, 0.5  $\mu$ M bCYB5, 1.000 U  $mL^{-1}$  catalase, 25 U  $mL^{-1}$  GDH, 20 mM glucose, 25  $\mu$ g  $mL^{-1}$  1,2-didodecanoyl-*sn*-glycero-3-phosphocholine (DLPC), 200  $\mu$ M substrate (from a 10 mM stock solution dissolved in DMSO), and 200  $\mu$ M NADP<sup>+</sup>. Samples were incubated as indicated in the results section for either 30 min, 90 min, or 24 h at 30 °C with 600 rpm shaking in a thermomixer C (Eppendorf, Hamburg, Germany).

Reactions containing saturated fatty acids 1–8 and *n*-alkanols 9–12 (group I and II) were stopped and acidified by addition of 2  $\mu$ L 37% HCl, followed by addition of 100  $\mu$ M of an internal standard. The substrates and their reaction products were extracted twice with 500  $\mu$ L tert-butyl-methyl ether (MTBE) by vortexing for 2 min and centrifugation for phase separation. The organic phases were pooled, dried with water-free  $MgSO_4$ , and evaporated. The residuals were resolved in 30  $\mu$ L N,O-bis(trimethylsilyl)trifluoroacetamide with 1% trimethylchlorosilane, incubated at 80 °C for 30 min, and subjected to GC/MS.

Reaction mixtures containing compounds of groups III–VII were extracted with 100  $\mu$ L ethyl acetate after addition of 100  $\mu$ M internal standard, and the organic phases were subjected to GC/MS.

Reaction mixtures containing compounds of groups VIII–X were extracted with 300  $\mu$ L ethyl acetate, the organic phases evaporated, and the residues dissolved in 30  $\mu$ L acetonitrile and subjected to LC/MS analysis.

All GC/MS, LC/MS, and LC/MS/MS methods used for individual compounds are listed in Supplementary Tables S4 and S5.

### 3.4. Screening for Compound-Induced Spectral Changes of CYP4B1

Screening of a natural product library (Screen-Well<sup>®</sup> Natural Product Library, BML-2865 Version 7.6; 502 compounds, Supplementary Table S1) was conducted in 96-well plates in a total volume of 100  $\mu$ L 50 mM  $KP_i$ , pH 7.5, with 0.4  $\mu$ M purified CYP4B1 and 2  $\mu$ L substrate (2 mg/mL in DMSO; concentration as provided by the Natural Product Library). After 5 min incubation, spectra were recorded between 360 nm and 480 nm on a plate reader (Infinite M200 PRO, Tecan, Männedorf, Switzerland). Reference spectra were obtained by measurement of samples in the absence of either the substrate (2  $\mu$ L DMSO instead) or CYP4B1. Potential binding spectra of two recordings for each compound were obtained by subtracting both reference spectra from the respective sample spectra. To avoid bias, the screening was performed blinded and by two different individuals.

### 3.5. Computational Methods

Homology models of CYP4B1 for the green monkey and mouse lemur were constructed on the basis of the crystal structure of the corresponding rabbit enzyme (pdb 5T6Q) using SWISS-MODEL [122–124].

For subsequent molecular docking, all ligand molecules were energetically optimized employing the build-in MM+ force field of HYPERCHEM version 8.0.10 (Hypercube Inc., Gainesville, FL, USA, 2011). AutoDock atom types and partial charges were computed with

an in-house PERL script. AutoDock Tools (Windows version 1.5.6r3) was used for further preparation of the ligands and the receptor structures [125].

Protonation states of the histidine residues were assigned by visual inspection in order to optimize their local hydrogen-bonding network. Partial charges for the receptor were generated as previously reported, also accounting for the changes caused by the covalent bond between the oxygen atom OE2 of Glu310 (5T6Q.pdb) and the carbon atom CMD of the heme-cofactor [126].

The rectangular grid box ( $74 \times 48 \times 56$  points) was chosen to be large enough to comprise the whole binding pocket. The grid spacing was kept at the default value of 0.375 Å, whereas the number of docking runs for the Lamarckian Genetic Algorithm was increased to the maximum value of 250. AutoDock version 4.2 was used to be consistent with our previous studies [127,128].

The protein part was kept rigid, but all rotatable bonds of the ligands were treated as flexible.

#### 4. Conclusions

Within our three-step approach based on spectral changes, *in vitro* conversions and computational methods, twenty-eight new substrates from eight groups were found, including terpenes, terpenoids, and aromatic and heterocyclic compounds, as well as stilbenoids and vanilloids. Furthermore, two reaction types that had so far not been observed for CYP4B1 were presented—with myristicin **41** a substrate undergoing an O-demethylation, and with thioanisole **34** an S-oxidation.

*In silico* docking and spectral changes present a good method for fast screening of large compound libraries; it should be noted, however, that these methods alone are not sufficient to achieve conclusive results, since in some cases false-positive results (meaning spectral changes indicating type I shift) were observed and false-negative results can also not be excluded. One example is quercetin **54**, which induced a clearly visible spectral change in the initial screening, but was not converted by CYP4B1 in the *in vitro* setup.

The comparison of the non-human primate orthologs chCYP4B1 and mlCYP4B1 with the well-investigated rabbit ortholog revealed several differences in substrate preferences with regard to catalytic activity, regioselectivity, and (in some cases) promiscuity. Generally, it can be stated that rCYP4B1 preferred smaller molecules (e.g., shorter chain-lengths of saturated fatty acids) and smaller cyclic molecules (e.g.,  $\alpha$ -pinene **26** and carvone **23**), whereas the primate CYP4B1 orthologs showed better acceptance for longer chain-lengths of saturated fatty acids and sterically more demanding compounds, including stilbene **42** and stilbenoids **43–45**, [6]-gingerol **49** and capsaicin **48**. Moreover, comparison of hydroxylation patterns of saturated fatty acids revealed that both primate orthologs have higher regioselectivity towards terminal  $\omega$ -hydroxylation, whereas rCYP4B1 is more promiscuous in terms of targeted hydroxylation positions. These observations suggest that CYP4B1 has undergone some changes during primate evolution that have an effect on its active site. However, a comparison of the crystal structure of rCYP4B1 with the homology models of chCYP4B1 and mlCYP4B1 revealed only one amino acid that is directly related to the active site, namely isoleucine at position 221 (rCYP4B1), which has mutated to a leucine at the corresponding position in chCYP4B1, and to a methionine in mlCYP4B1. Since crystal structures of the primate orthologs are not yet available, we can only discuss these results based on homology modeling. Although the structural identity to rCYP4B1 in both primate orthologs is about 85% (and 89% to each other), it cannot be excluded that the sequence differences outside the active site can also lead to structural changes that have an influence on the active site but cannot be seen in the modeling.

In conclusion, our results demonstrate that CYP4B1 acting at the interface between endobiotic and xenobiotic metabolism is a far more promiscuous enzyme than previously thought. The differences in activity observed across the three investigated species indicate that CYP4B1 has undergone evolutionary changes ultimately leading to a complete loss of catalytic function in humans. Further investigations should therefore focus on these evolutionary aspects.

**Supplementary Materials:** The following supporting information can be downloaded at: <https://www.mdpi.com/article/10.3390/catal15050454/s1>, Table S1: screening results of the Natural Product Library Screen-Well® Natural Product Library, BML-2865 Version 7.6; Table S2: product distribution obtained with saturated fatty acids; Table S3: product distribution obtained with *n*-alkanols; Table S4: summary of GC/MS methods; Table S5: summary of LC/MS methods; Table S6: expression yields; Figure S1: CYP4B1 expression in *E. coli*; synthetic gene sequences.

**Author Contributions:** Conceptualization, M.G. and A.R.; methodology, A.R. and M.C.H.; validation, A.R., M.C.H., S.H., C.W. and M.G.; formal analysis, A.R., M.C.H., E.H. and P.J.F.; investigation, A.R., M.C.H., E.H. and P.J.F.; data curation, A.R.; writing—original draft preparation, A.R.; writing—review and editing, A.R., M.C.H., S.H., C.W. and M.G.; visualization, A.R. and M.C.H.; supervision, M.G. and C.W.; project administration, M.G.; funding acquisition, M.G. and C.W. All authors have read and agreed to the published version of the manuscript.

**Funding:** This research was funded by the Deutsche Forschungsgemeinschaft (DFG), grant number GI 1423/2-1 awarded to Marco Girhard, and grant number WI 5377/2-1 awarded to Constanze Wiek.

**Data Availability Statement:** The original contributions presented in this study are included in the article/Supplementary Material. Further inquiries can be directed to the corresponding author.

**Acknowledgments:** We wish to thank Rita Bernhardt, Saarland University, Saarbruecken (Germany), for kindly providing us with the Natural Product Library and the plasmid for Cytochrome *b*<sub>5</sub> expression. We would also like to thank Birgit Henßen and Elias Pfirrmann, Institute of Bioorganic Chemistry, Heinrich Heine University Düsseldorf, Forschungszentrum Jülich GmbH (Germany), for their collaboration in the enantiomer separation of sulfoxides.

**Conflicts of Interest:** The authors declare no conflicts of interest.

## References

1. Lamb, D.C.; Follmer, A.H.; Goldstone, J.V.; Nelson, D.R.; Warrilow, A.G.; Price, C.L.; True, M.Y.; Kelly, S.L.; Poulos, T.L.; Stegeman, J.J. On the occurrence of cytochrome P450 in viruses. *Proc. Natl. Acad. Sci. USA* **2019**, *116*, 12343–12352. [[CrossRef](#)]
2. Nelson, D.R. Cytochrome P450 diversity in the tree of life. *Biochim. Biophys. Acta Proteins Proteom.* **2018**, *1866*, 141–154. [[CrossRef](#)]
3. Akhtar, M.; Wright, J. A unified mechanistic view of oxidative reactions catalysed by P-450 and related Fe-containing enzymes. *Nat. Prod. Rep.* **1991**, *8*, 527–551. [[CrossRef](#)]
4. Bernhardt, R.; Urlacher, V.B. Cytochromes P450 as promising catalysts for biotechnological application: Chances and limitations. *Appl. Microbiol. Biotechnol.* **2014**, *98*, 6185–6203. [[CrossRef](#)] [[PubMed](#)]
5. Bhattacharya, S.S.; Yadav, J.S. Microbial P450 enzymes in bioremediation and drug discovery: Emerging potentials and challenges. *Curr. Protein Pept. Sci.* **2018**, *19*, 75–86. [[CrossRef](#)] [[PubMed](#)]
6. Urlacher, V.B.; Girhard, M. Cytochrome P450 monooxygenases: An update on perspectives for synthetic application. *Trends Biotechnol.* **2012**, *30*, 26–36. [[CrossRef](#)] [[PubMed](#)]
7. Urlacher, V.B.; Girhard, M. Cytochrome P450 Monooxygenases in Biotechnology and Synthetic Biology. *Trends Biotechnol.* **2019**, *37*, 882–897. [[CrossRef](#)]
8. Nelson, D.R.; Kamataki, T.; Waxman, D.J.; Guengerich, F.P.; Estabrook, R.W.; Feyereisen, R.; Gonzalez, F.J.; Coon, M.J.; Gunsalus, I.C.; Gotoh, O.; et al. The P450 Superfamily: Update on New Sequences, Gene Mapping, Accession Numbers, Early Trivial Names of Enzymes, and Nomenclature. *DNA Cell Biol.* **1993**, *12*, 1–51. [[CrossRef](#)]
9. Hsu, M.H.; Savas, U.; Griffin, K.J.; Johnson, E.F. Human cytochrome p450 family 4 enzymes: Function, genetic variation and regulation. *Drug Metab. Rev.* **2007**, *39*, 515–538. [[CrossRef](#)]
10. Simpson, A.E.C.M. The cytochrome P450 4 (CYP4) family. *Gen. Pharmacol. Vasc. Syst.* **1997**, *28*, 351–359. [[CrossRef](#)]

11. Baer, B.R.; Rettie, A.E. CYP4B1: An enigmatic P450 at the interface between xenobiotic and endobiotic metabolism. *Drug Metab. Rev.* **2006**, *38*, 451–476. [[CrossRef](#)] [[PubMed](#)]
12. Hardwick, J.P. Cytochrome P450 omega hydroxylase (CYP4) function in fatty acid metabolism and metabolic diseases. *Biochem. Pharmacol.* **2008**, *75*, 2263–2275. [[CrossRef](#)] [[PubMed](#)]
13. Röder, A.; Hüsken, S.; Hutter, M.C.; Rettie, A.E.; Hanenberg, H.; Wiek, C.; Girhard, M. Spotlight on CYP4B1. *Int. J. Mol. Sci.* **2023**, *24*, 2038. [[CrossRef](#)]
14. Thesseling, F.A.; Hutter, M.C.; Wiek, C.; Kowalski, J.P.; Rettie, A.E.; Girhard, M. Novel insights into oxidation of fatty acids and fatty alcohols by cytochrome P450 monooxygenase CYP4B1. *Arch. Biochem. Biophys.* **2020**, *679*, 108216. [[CrossRef](#)]
15. Scott, E.E. omega- versus (omega-1)-hydroxylation: Cytochrome P450 4B1 sterics make the call. *J. Biol. Chem.* **2017**, *292*, 5622–5623. [[CrossRef](#)]
16. Boyd, M.R.; Burka, L.T.; Harris, T.M.; Willson, B.J. Lung-toxic furanoterpenoids produced by sweet potatoes (*Ipomoea batatas*) following microbial infection. *Biochim. Biophys. Acta (BBA)-Lipids Lipid Metab.* **1974**, *337*, 184–195. [[CrossRef](#)]
17. Wilson, B.J.; Yang, D.T.; Boyd, M.R. Toxicity of mould-damaged sweet potatoes (*Ipomoea batatas*). *Nature* **1970**, *227*, 521–522. [[CrossRef](#)]
18. Garst, J.; Wilson, W.; Kristensen, N.; Harrison, P.; Corbin, J.; Simon, J.; Philpot, R.; Szabo, R. Species susceptibility to the pulmonary toxicity of 3-furyl isoamyl ketone (perilla ketone): In vivo support for involvement of the lung monooxygenase system. *J. Anim. Sci.* **1985**, *60*, 248–257. [[CrossRef](#)] [[PubMed](#)]
19. Devereux, T.R.; Jones, K.G.; Bend, J.R.; Fouts, J.R.; Statham, C.N.; Boyd, M.R. In vitro metabolic activation of the pulmonary toxin, 4-ipomeanol, in nonciliated bronchioal epithelial (Clara) and alveolar type ii cells isolated from rabbit lung. *J. Pharmacol. Exp. Ther.* **1981**, *220*, 223–227. [[CrossRef](#)]
20. Slaughter, S.R.; Statham, C.N.; Philpot, R.M.; Boyd, M.R. Covalent binding of metabolites of 4-ipomeanol to rabbit pulmonary and hepatic microsomal proteins and to the enzymes of the pulmonary cytochrome P-450-dependent monooxygenase system. *J. Pharmacol. Exp. Ther.* **1983**, *224*, 252–257. [[CrossRef](#)]
21. Smith, P.B.; Tiano, H.F.; Nesnow, S.; Boyd, M.R.; Philpot, R.M.; Langenbach, R. 4-*Ipomeanol* and 2-aminoanthracene cytotoxicity in C3H/10T12 cells expressing rabbit cytochrome P450 4B1. *Biochem. Pharmacol.* **1995**, *50*, 1567–1575. [[CrossRef](#)] [[PubMed](#)]
22. Wilson, B.J.; Garst, J.E.; Linnabary, R.D.; Channell, R.B. Perilla ketone: A potent lung toxin from the mint plant, *Perilla frutescens* Britton. *Science* **1977**, *197*, 573–574. [[CrossRef](#)]
23. Roellecke, K.; Jager, V.D.; Gyurov, V.H.; Kowalski, J.P.; Mielke, S.; Rettie, A.E.; Hanenberg, H.; Wiek, C.; Girhard, M. Ligand characterization of CYP4B1 isoforms modified for high-level expression in *Escherichia coli* and HepG2 cells. *Protein Eng. Des. Sel.* **2017**, *30*, 205–216. [[CrossRef](#)]
24. Kowalski, J.P.; McDonald, M.G.; Whittington, D.; Guttman, M.; Scian, M.; Girhard, M.; Hanenberg, H.; Wiek, C.; Rettie, A.E. Structure-Activity Relationships for CYP4B1 Bioactivation of 4-*Ipomeanol* Congeners: Direct Correlation between Cytotoxicity and Trapped Reactive Intermediates. *Chem. Res. Toxicol.* **2019**, *32*, 2488–2498. [[CrossRef](#)]
25. Johannessen, C.U.; Johannessen, S.I. Valproate: Past, present, and future. *CNS Drug Rev.* **2003**, *9*, 199–216. [[CrossRef](#)]
26. Rettie, A.E.; Sheffels, P.R.; Korzekwa, K.R.; Gonzalez, F.J.; Philpot, R.M.; Baillie, T.A. CYP4 isoenzyme specificity and the relationship between. Omega-hydroxylation and terminal desaturation of valproic acid. *Biochemistry* **1995**, *34*, 7889–7895. [[CrossRef](#)] [[PubMed](#)]
27. Baer, B.R.; Rettie, A.E.; Henne, K.R. Bioactivation of 4-*ipomeanol* by CYP4B1: Adduct characterization and evidence for an enedial intermediate. *Chem. Res. Toxicol.* **2005**, *18*, 855–864. [[CrossRef](#)] [[PubMed](#)]
28. Frank, S.; Steffens, S.; Fischer, U.; Tlolko, A.; Rainov, N.G.; Kramm, C.M. Differential cytotoxicity and bystander effect of the rabbit cytochrome P450 4B1 enzyme gene by two different prodrugs: Implications for pharmacogene therapy. *Cancer Gene Ther.* **2002**, *9*, 178–188. [[CrossRef](#)]
29. Zheng, Y.-M.; Fisher, M.B.; Yokotani, N.; Fujii-Kuriyama, Y.; Rettie, A.E. Identification of a meander region proline residue critical for heme binding to cytochrome P450: Implications for the catalytic function of human CYP4B1. *Biochemistry* **1998**, *37*, 12847–12851. [[CrossRef](#)]
30. Zheng, Y.-M.; Henne, K.R.; Charmley, P.; Kim, R.B.; McCarver, D.G.; Cabacungan, E.T.; Hines, R.N.; Rettie, A.E. Genotyping and site-directed mutagenesis of a cytochrome P450 meander Pro-X-Arg motif critical to CYP4B1 catalysis. *Toxicol. Appl. Pharmacol.* **2003**, *186*, 119–126. [[CrossRef](#)]
31. Lim, S.; Alshagga, M.; Ong, C.E.; Chieng, J.Y.; Pan, Y. Cytochrome P450 4B1 (CYP4B1) as a target in cancer treatment. *Hum. Exp. Toxicol.* **2020**, *39*, 785–796. [[CrossRef](#)] [[PubMed](#)]
32. Czerwinski, M.; McLemore, T.L.; Gelboin, H.V.; Gonzalez, F.J. Quantification of CYP2B7, CYP4B1, and CYPOR messenger RNAs in normal human lung and lung tumors. *Cancer Res.* **1994**, *54*, 1085–1091. [[PubMed](#)]
33. Barlin, J.N.; Jelinic, P.; Olvera, N.; Bogomolny, F.; Bisogna, M.; Dao, F.; Barakat, R.R.; Chi, D.S.; Levine, D.A. Validated gene targets associated with curatively treated advanced serous ovarian carcinoma. *Gynecol. Oncol.* **2013**, *128*, 512–517. [[CrossRef](#)] [[PubMed](#)]

34. Imaoka, S.; Yoneda, Y.; Sugimoto, T.; Hiroi, T.; Yamamoto, K.; Nakatani, T.; Funae, Y. CYP4B1 is a possible risk factor for bladder cancer in humans. *Biochem. Biophys. Res. Commun.* **2000**, *277*, 776–780. [[CrossRef](#)]
35. Lin, J.T.; Chan, T.C.; Li, C.F.; Huan, S.K.H.; Tian, Y.F.; Liang, P.I.; Pan, C.T.; Shiue, Y.L. Downregulation of the cytochrome P450 4B1 protein confers a poor prognostic factor in patients with urothelial carcinomas of upper urinary tracts and urinary bladder. *APMIS* **2019**, *127*, 170–180. [[CrossRef](#)]
36. Schenkman, J.B. Nature of the type I and II spectral changes in liver microsomes. *Biochemistry* **1970**, *9*, 2081–2091. [[CrossRef](#)]
37. Denisov, I.G.; Makris, T.M.; Sligar, S.G.; Schlichting, I. Structure and Chemistry of Cytochrome P450. *Chem. Rev.* **2005**, *105*, 2253–2278. [[CrossRef](#)]
38. Adams, T.B.; Gavin, C.L.; McGowen, M.M.; Waddell, W.J.; Cohen, S.M.; Feron, V.J.; Marnett, L.J.; Munro, I.C.; Portoghese, P.S.; Rietjens, I.M.; et al. The FEMA GRAS assessment of aliphatic and aromatic terpene hydrocarbons used as flavor ingredients. *Food Chem. Toxicol.* **2011**, *49*, 2471–2494. [[CrossRef](#)]
39. Bogazkaya, A.M.; von Bühler, C.J.; Kriening, S.; Busch, A.; Seifert, A.; Pleiss, J.; Laschat, S.; Urlacher, V.B. Selective allylic hydroxylation of acyclic terpenoids by CYP154E1 from *Thermobifida fusca* YX. *Beilstein J. Org. Chem.* **2014**, *10*, 1347–1353. [[CrossRef](#)]
40. von Bühler, C.; Le-Huu, P.; Urlacher, V.B. Cluster screening: An effective approach for probing the substrate space of uncharacterized cytochrome P450s. *Chembiochem* **2013**, *14*, 2189–2198. [[CrossRef](#)]
41. Hagvall, L.; Baron, J.M.; Borje, A.; Weidolf, L.; Merk, H.; Karlberg, A.T. Cytochrome P450-mediated activation of the fragrance compound geraniol forms potent contact allergens. *Toxicol. Appl. Pharmacol.* **2008**, *233*, 308–313. [[CrossRef](#)]
42. Shimada, T.; Shindo, M.; Miyazawa, M. Species differences in the metabolism of (+)- and (–)-limonenes and their metabolites, carveols and carvones, by cytochrome P450 enzymes in liver microsomes of mice, rats, guinea pigs, rabbits, dogs, monkeys, and humans. *Drug Metab. Pharmacokinet.* **2002**, *17*, 507–515. [[CrossRef](#)]
43. Yoshida, E.; Kojima, M.; Suzuki, M.; Matsuda, F.; Shimbo, K.; Onuki, A.; Nishio, Y.; Usuda, Y.; Kondo, A.; Ishii, J. Increased carvone production in *Escherichia coli* by balancing limonene conversion enzyme expression via targeted quantification concatamer proteome analysis. *Sci. Rep.* **2021**, *11*, 22126. [[CrossRef](#)]
44. Hedenstierna, G.; Alexandersson, R.; Wimander, K.; Rosén, G. Exposure to terpenes: Effects on pulmonary function. *Int. Arch. Occup. Environ. Health* **1983**, *51*, 191–198. [[CrossRef](#)]
45. Eriksson, K.; Levin, J.-O. Identification of cis- and trans-verbenol in human urine after occupational exposure to terpenes. *Int. Arch. Occup. Environ. Health* **1990**, *62*, 379–383. [[CrossRef](#)]
46. Ishida, T.; Asakawa, Y.; Takemoto, T.; Aratani, T. Terpenoids biotransformation in mammals III: Biotransformation of alpha-pinene, beta-pinene, pinane, 3-carene, carane, myrcene, and p-cymene in rabbits. *J. Pharm. Sci.* **1981**, *70*, 406–415. [[CrossRef](#)]
47. Schmidt, L.; Goen, T. Human metabolism of alpha-pinene and metabolite kinetics after oral administration. *Arch. Toxicol.* **2017**, *91*, 677–687. [[CrossRef](#)] [[PubMed](#)]
48. Moorthy, B.; Chu, C.; Carlin, D.J. Polycyclic aromatic hydrocarbons: From metabolism to lung cancer. *Toxicol. Sci.* **2015**, *145*, 5–15. [[CrossRef](#)]
49. Reid, B.C.; Ghazarian, A.A.; DeMarini, D.M.; Sapkota, A.; Jack, D.; Lan, Q.; Winn, D.M.; Birnbaum, L.S. Research opportunities for cancer associated with indoor air pollution from solid-fuel combustion. *Environ. Health Perspect.* **2012**, *120*, 1495–1498. [[CrossRef](#)]
50. Piccardo, M.T.; Stella, A.; Valerio, F. Is the smokers exposure to environmental tobacco smoke negligible? *Environ. Health* **2010**, *9*, 5. [[CrossRef](#)]
51. Boström, C.E.; Gerde, P.; Hanberg, A.; Jernström, B.; Johansson, C.; Kyrklund, T.; Rannug, A.; Törnqvist, M.; Victorin, K.; Westerholm, R. Cancer risk assessment, indicators, and guidelines for polycyclic aromatic hydrocarbons in the ambient air. *Environ. Health Perspect.* **2002**, *110* (Suppl. 3), 451–488. [[CrossRef](#)]
52. Heibati, B.; Renz, H.; Lacy, P. Wildfire and wood smoke effects on human airway epithelial cells: A scoping review. *Environ. Res.* **2025**, *272*, 121153. [[CrossRef](#)]
53. Stading, R.; Gastelum, G.; Chu, C.; Jiang, W.; Moorthy, B. Molecular mechanisms of pulmonary carcinogenesis by polycyclic aromatic hydrocarbons (PAHs): Implications for human lung cancer. *Semin. Cancer Biol.* **2021**, *76*, 3–16. [[CrossRef](#)]
54. Chen, L.J.; Wegerski, C.J.; Kramer, D.J.; Thomas, L.A.; McDonald, J.D.; Dix, K.J.; Sanders, J.M. Disposition and metabolism of cumene in F344 rats and B6C3F1 mice. *Drug Metab. Dispos.* **2011**, *39*, 498–509. [[CrossRef](#)]
55. Henne, K.R.; Fisher, M.B.; Iyer, K.R.; Lang, D.H.; Trager, W.F.; Rettie, A.E. Active site characteristics of CYP4B1 probed with aromatic ligands. *Biochemistry* **2001**, *40*, 8597–8605. [[CrossRef](#)]
56. Li, Y.; Ma, Y.; Li, P.; Zhang, X.; Ribitsch, D.; Alcalde, M.; Hollmann, F.; Wang, Y. Enantioselective Sulfoxidation of Thioanisole by Cascading a Choline Oxidase and a Peroxygenase in the Presence of Natural Deep Eutectic Solvents. *Chempluschem* **2020**, *85*, 254–257. [[CrossRef](#)]
57. Yin, Y.C.; Yu, H.L.; Luan, Z.J.; Li, R.J.; Ouyang, P.F.; Liu, J.; Xu, J.H. Unusually broad substrate profile of self-sufficient cytochrome P450 monooxygenase CYP116B4 from *Labrenzia aggregata*. *Chembiochem* **2014**, *15*, 2443–2449. [[CrossRef](#)]

58. Fruetel, J.A.; Mackman, R.L.; Peterson, J.A.; Ortiz de Montellano, P.R. Relationship of active site topology to substrate specificity for cytochrome P450terp (CYP108). *J. Biol. Chem.* **1994**, *269*, 28815–28821. [[CrossRef](#)]
59. Song, Y.; Wang, Y.; Pan, B.; Cheng, X.; Yang, J.; Chen, Y. Recent Advances in Biocatalytic Preparation of Chiral Sulfoxides. *Asian J. Org. Chem.* **2025**, *14*, e202400708. [[CrossRef](#)]
60. Fruetel, J.; Chang, Y.-T.; Collins, J.; Loew, G.; Ortiz de Montellano, P.R. Thioanisole Sulfoxidation by Cytochrome P450cam (CYP101): Experimental and Calculated Absolute Stereochemistries. *J. Am. Chem. Soc.* **1994**, *116*, 11643–11648. [[CrossRef](#)]
61. West, J.A.A.; Pakehham, G.; Morin, D.; Fleschner, C.A.; Buckpitt, A.R.; Plopper, C.G. Inhaled Naphthalene Causes Dose Dependent Clara Cell Cytotoxicity in Mice but Not in Rats. *Toxicol. Appl. Pharmacol.* **2001**, *173*, 114–119. [[CrossRef](#)]
62. Plopper, C.G.; Suverkropp, C.; Morin, D.; Nishio, S.; Buckpitt, A. Relationship of cytochrome P-450 activity to Clara cell cytotoxicity. I. Histopathologic comparison of the respiratory tract of mice, rats and hamsters after parenteral administration of naphthalene. *J. Pharmacol. Exp. Ther.* **1992**, *261*, 353–363. [[CrossRef](#)]
63. Cohen, J.T.; Carlson, G.; Charnley, G.; Coggon, D.; Delzell, E.; Graham, J.D.; Greim, H.; Krewski, D.; Medinsky, M.; Monson, R.; et al. A comprehensive evaluation of the potential health risks associated with occupational and environmental exposure to styrene. *J. Toxicol. Environ. Health-Part B Crit. Rev.* **2002**, *5*, 1–263. [[CrossRef](#)]
64. Gadberry, M.G.; DeNicola, D.B.; Carlson, G.P. Pneumotoxicity and hepatotoxicity of styrene and styrene oxide. *J. Toxicol. Environ. Health* **1996**, *48*, 273–294. [[CrossRef](#)]
65. Bhurta, D.; Bharate, S.B. Styryl Group, a Friend or Foe in Medicinal Chemistry. *ChemMedChem* **2022**, *17*, e202100706. [[CrossRef](#)]
66. Elbarbry, F.; Espiritu, M.J.; Soo, K.; Yee, B.; Taylor, J. Inhibition of soluble epoxide hydrolase by natural isothiocyanates. *Biochem. Biophys. Res. Commun.* **2024**, *725*, 150261. [[CrossRef](#)]
67. Fretland, A.J.; Omiecinski, C.J. Epoxide hydrolases: Biochemistry and molecular biology. *Chem.-Biol. Interact.* **2000**, *129*, 41–59. [[CrossRef](#)]
68. Shen, S.; Li, L.; Ding, X.; Zheng, J. Metabolism of styrene to styrene oxide and vinylphenols in cytochrome P450 2F2- and P450 2E1-knockout mouse liver and lung microsomes. *Chem. Res. Toxicol.* **2014**, *27*, 27–33. [[CrossRef](#)] [[PubMed](#)]
69. Carlson, G.P. Comparison of the susceptibility of wild-type and CYP2E1 knockout mice to the hepatotoxic and pneumotoxic effects of styrene and styrene oxide. *Toxicol. Lett.* **2004**, *150*, 335–339. [[CrossRef](#)]
70. Li, Q.S.; Ogawa, J.; Schmid, R.D.; Shimizu, S. Engineering cytochrome P450 BM-3 for oxidation of polycyclic aromatic hydrocarbons. *Appl. Environ. Microbiol.* **2001**, *67*, 5735–5739. [[CrossRef](#)]
71. Baldwin, R.M.; Shultz, M.A.; Buckpitt, A.R. Bioactivation of the pulmonary toxicants naphthalene and 1-nitronaphthalene by rat CYP2F4. *J. Pharmacol. Exp. Ther.* **2005**, *312*, 857–865. [[CrossRef](#)]
72. Boyd, M.R.; Wilson, B.J. Isolation and characterization of 4-ipomeanol, a lung-toxic furanoterpenoid produced by sweet potatoes (*Ipomoea batatas*). *J. Agric. Food Chem.* **1972**, *20*, 428–430. [[CrossRef](#)]
73. Czerwinski, M.; McLemore, T.L.; Philpot, R.M.; Nhamburo, P.T.; Korzekwa, K.; Gelboin, H.V.; Gonzalez, F.J. Metabolic activation of 4-ipomeanol by complementary DNA-expressed human cytochromes P-450: Evidence for species-specific metabolism. *Cancer Res.* **1991**, *51*, 4636–4638. [[PubMed](#)]
74. Wu, Z.L.; Podust, L.M.; Guengerich, F.P. Expansion of substrate specificity of cytochrome P450 2A6 by random and site-directed mutagenesis. *J. Biol. Chem.* **2005**, *280*, 41090–41100. [[CrossRef](#)] [[PubMed](#)]
75. Kunevicius, A.; Sadauskas, M.; Raudyte, J.; Meskys, R.; Burokas, A. Unraveling the Dynamics of Host-Microbiota Indole Metabolism: An Investigation of Indole, Indolin-2-one, Isatin, and 3-Hydroxyindolin-2-one. *Molecules* **2024**, *29*, 993. [[CrossRef](#)] [[PubMed](#)]
76. Carpenedo, R.; Mannaioni, G.; Moroni, F. Oxindole, a sedative tryptophan metabolite, accumulates in blood and brain of rats with acute hepatic failure. *J. Neurochem.* **1998**, *70*, 1998–2003. [[CrossRef](#)]
77. Jaglin, M.; Rhimi, M.; Philippe, C.; Pons, N.; Bruneau, A.; Goustard, B.; Dauge, V.; Maguin, E.; Naudon, L.; Rabot, S. Indole, a Signaling Molecule Produced by the Gut Microbiota, Negatively Impacts Emotional Behaviors in Rats. *Front. Neurosci.* **2018**, *12*, 216. [[CrossRef](#)]
78. D'Agostino, J.; Zhuo, X.; Shadid, M.; Morgan, D.G.; Zhang, X.; Humphreys, W.G.; Shu, Y.Z.; Yost, G.S.; Ding, X. The pneumotoxin 3-methylindole is a substrate and a mechanism-based inactivator of CYP2A13, a human cytochrome P450 enzyme preferentially expressed in the respiratory tract. *Drug Metab. Dispos.* **2009**, *37*, 2018–2027. [[CrossRef](#)]
79. Yost, G.S. Bioactivation of Toxicants by Cytochrome P450-Mediated Dehydrogenation Mechanisms. In *Biological Reactive Intermediates VI: Chemical and Biological Mechanisms in Susceptibility to and Prevention of Environmental Diseases*; Dansette, P.M., Snyder, R., Delaforge, M., Gibson, G.G., Greim, H., Jollow, D.J., Monks, T.J., Sipes, I.G., Eds.; Springer: Boston, MA, USA, 2001; pp. 53–62. [[CrossRef](#)]
80. Skiles, G.L.; Yost, G.S. Mechanistic studies on the cytochrome P450-catalyzed dehydrogenation of 3-methylindole. *Chem. Res. Toxicol.* **1996**, *9*, 291–297. [[CrossRef](#)]
81. Haydock, L.A.J.; Fenton, R.K.; Sergejewich, L.; Squires, E.J.; Caswell, J.L. Acute interstitial pneumonia and the biology of 3-methylindole in feedlot cattle. *Anim. Health Res. Rev.* **2022**, *23*, 72–81. [[CrossRef](#)]

82. Yost, G.S. Mechanisms of 3-methylindole pneumotoxicity. *Chem. Res. Toxicol.* **1989**, *2*, 273–279. [[CrossRef](#)]
83. Lichtenstein, E.P.; Casida, J.E. Naturally Occurring Insecticides, Myristicin, an Insecticide and Synergist Occurring Naturally in the Edible Parts of Parsnips. *J. Agric. Food Chem.* **1963**, *11*, 410–415. [[CrossRef](#)]
84. Götz, M.E.; Sachse, B.; Schäfer, B.; Eisenreich, A. Myristicin and Elemicin: Potentially Toxic Alkenylbenzenes in Food. *Foods* **2022**, *11*, 1988. [[CrossRef](#)] [[PubMed](#)]
85. Kaur, V.; Kaushal, S.; Utreja, D. Occurrence, Isolation, Pharmacological Potential, Metabolism, and Toxicity of Myristicin: A Naturally Occurring Alkoxy-Substituted Allylbenzene. *Mini-Rev. Org. Chem.* **2024**, *21*, 477–493. [[CrossRef](#)]
86. Zhu, X.; Wang, Y.K.; Yang, X.N.; Xiao, X.R.; Zhang, T.; Yang, X.W.; Qin, H.B.; Li, F. Metabolic Activation of Myristicin and Its Role in Cellular Toxicity. *J. Agric. Food Chem.* **2019**, *67*, 4328–4336. [[CrossRef](#)]
87. Yun, C.-H.; Lee, H.S.; Lee, H.-Y.; Yim, S.-K.; Kim, K.-H.; Kim, E.; Yea, S.-S.; Guengerich, F.P. Roles of human liver cytochrome P450 3A4 and 1A2 enzymes in the oxidation of myristicin. *Toxicol. Lett.* **2003**, *137*, 143–150. [[CrossRef](#)]
88. Rietjens, I.M.; Cohen, S.M.; Fukushima, S.; Gooderham, N.J.; Hecht, S.; Marnett, L.J.; Smith, R.L.; Adams, T.B.; Bastaki, M.; Harman, C.G.; et al. Impact of structural and metabolic variations on the toxicity and carcinogenicity of hydroxy- and alkoxy-substituted allyl- and propenylbenzenes. *Chem. Res. Toxicol.* **2014**, *27*, 1092–1103. [[CrossRef](#)]
89. Akinwumi, B.C.; Bordun, K.M.; Anderson, H.D. Biological Activities of Stilbenoids. *Int. J. Mol. Sci.* **2018**, *19*, 792. [[CrossRef](#)]
90. Mattio, L.M.; Catinella, G.; Dallavalle, S.; Pinto, A. Stilbenoids: A Natural Arsenal against Bacterial Pathogens. *Antibiotics* **2020**, *9*, 336. [[CrossRef](#)]
91. Maccario, C.; Savio, M.; Ferraro, D.; Bianchi, L.; Pizzala, R.; Pretali, L.; Forti, L.; Stivala, L.A. The resveratrol analog 4,4'-dihydroxy-trans-stilbene suppresses transformation in normal mouse fibroblasts and inhibits proliferation and invasion of human breast cancer cells. *Carcinogenesis* **2012**, *33*, 2172–2180. [[CrossRef](#)]
92. Smoliga, J.M.; Baur, J.A.; Hausenblas, H.A. Resveratrol and health—A comprehensive review of human clinical trials. *Mol. Nutr. Food Res.* **2011**, *55*, 1129–1141. [[CrossRef](#)]
93. Liu, J.; Sridhar, J.; Foroozesh, M. Cytochrome P450 family 1 inhibitors and structure-activity relationships. *Molecules* **2013**, *18*, 14470–14495. [[CrossRef](#)] [[PubMed](#)]
94. Sanoh, S.; Kitamura, S.; Sugihara, K.; Ohta, S. Cytochrome P450 1A1/2 mediated metabolism of trans-stilbene in rats and humans. *Biol. Pharm. Bull.* **2002**, *25*, 397–400. [[CrossRef](#)] [[PubMed](#)]
95. Savio, M.; Ferraro, D.; Maccario, C.; Vaccarone, R.; Jensen, L.D.; Corana, F.; Mannucci, B.; Bianchi, L.; Cao, Y.; Stivala, L.A. Resveratrol analogue 4,4'-dihydroxy-trans-stilbene potently inhibits cancer invasion and metastasis. *Sci. Rep.* **2016**, *6*, 19973. [[CrossRef](#)] [[PubMed](#)]
96. Kimura, Y.; Sumiyoshi, M.; Kiyoi, T.; Baba, K. Dihydroxystilbenes prevent azoxymethane/dextran sulfate sodium-induced colon cancer by inhibiting colon cytokines, a chemokine, and programmed cell death-1 in C57BL/6J mice. *Eur. J. Pharmacol.* **2020**, *886*, 173445. [[CrossRef](#)]
97. Torres, P.; Avila, J.G.; Romo de Vivar, A.; Garcia, A.M.; Marin, J.C.; Aranda, E.; Cespedes, C.L. Antioxidant and insect growth regulatory activities of stilbenes and extracts from *Yucca periculosa*. *Phytochemistry* **2003**, *64*, 463–473. [[CrossRef](#)]
98. Beltrán, L.R.; Dawid, C.; Beltrán, M.; Gisselmann, G.; Degenhardt, K.; Mathie, K.; Hofmann, T.; Hatt, H. The pungent substances piperine, capsaicin, 6-gingerol and polygodial inhibit the human two-pore domain potassium channels TASK-1, TASK-3 and TRESK. *Front. Pharmacol.* **2013**, *4*, 141. [[CrossRef](#)]
99. Caterina, M.J.; Schumacher, M.A.; Tominaga, M.; Rosen, T.A.; Levine, J.D.; Julius, D. The capsaicin receptor: A heat-activated ion channel in the pain pathway. *Nature* **1997**, *389*, 816–824. [[CrossRef](#)]
100. Dedov, V.N.; Tran, V.H.; Duke, C.C.; Connor, M.; Christie, M.J.; Mandadi, S.; Roufogalis, B.D. Gingerols: A novel class of vanilloid receptor (VR1) agonists. *Br. J. Pharmacol.* **2002**, *137*, 793–798. [[CrossRef](#)]
101. Correa, E.A.; Hogestatt, E.D.; Sterner, O.; Echeverri, F.; Zygmunt, P.M. In vitro TRPV1 activity of piperine derived amides. *Bioorg Med. Chem.* **2010**, *18*, 3299–3306. [[CrossRef](#)]
102. Dawid, C.; Henze, A.; Frank, O.; Glabasnia, A.; Rupp, M.; Buning, K.; Orlikowski, D.; Bader, M.; Hofmann, T. Structural and sensory characterization of key pungent and tingling compounds from black pepper (*Piper nigrum* L.). *J. Agric. Food Chem.* **2012**, *60*, 2884–2895. [[CrossRef](#)]
103. Reilly, C.A.; Henion, F.; Bugni, T.S.; Ethirajan, M.; Stockmann, C.; Pramanik, K.C.; Srivastava, S.K.; Yost, G.S. Reactive intermediates produced from the metabolism of the vanilloid ring of capsaicinoids by p450 enzymes. *Chem. Res. Toxicol.* **2013**, *26*, 55–66. [[CrossRef](#)] [[PubMed](#)]
104. Reilly, C.A.; Yost, G.S. Metabolism of capsaicinoids by P450 enzymes: A review of recent findings on reaction mechanisms, bio-activation, and detoxification processes. *Drug Metab. Rev.* **2006**, *38*, 685–706. [[CrossRef](#)] [[PubMed](#)]
105. Surh, Y.-J.; Sup Lee, S. Capsaicin, a double-edged sword: Toxicity, metabolism, and chemopreventive potential. *Life Sci.* **1995**, *56*, 1845–1855. [[CrossRef](#)] [[PubMed](#)]
106. Cheng, J.; Yang, X.N.; Liu, X.; Zhang, S.P. Capsaicin for allergic rhinitis in adults. *Cochrane Database Syst. Rev.* **2006**, *2006*, CD004460. [[CrossRef](#)]

107. Derebery, M.J.; Dicpinigaitis, P.V. New horizons: Current and potential future self-treatments for acute upper respiratory tract conditions. *Postgrad. Med.* **2013**, *125*, 82–96. [[CrossRef](#)]
108. Chen, C.; Chen, X.; Mo, Q.; Liu, J.; Yao, X.; Di, X.; Qin, Z.; He, L.; Yao, Z. Cytochrome P450 metabolism studies of [6]-gingerol, [8]-gingerol, and [10]-gingerol by liver microsomes of humans and different species combined with expressed CYP enzymes. *RSC Adv.* **2023**, *13*, 5804–5812. [[CrossRef](#)]
109. Reilly, C.A.; Ehlhardt, W.J.; Jackson, D.A.; Kulanthaivel, P.; Mutlib, A.E.; Espina, R.J.; Moody, D.E.; Crouch, D.J.; Yost, G.S. Metabolism of capsaicin by cytochrome P450 produces novel dehydrogenated metabolites and decreases cytotoxicity to lung and liver cells. *Chem. Res. Toxicol.* **2003**, *16*, 336–349. [[CrossRef](#)]
110. Zhang, W.; Zhang, Y.; Fan, J.; Feng, Z.; Song, X. Pharmacological activity of capsaicin: Mechanisms and controversies (Review). *Mol. Med. Rep.* **2024**, *29*, 38. [[CrossRef](#)]
111. Nagayoshi, H.; Murayama, N.; Kim, V.; Kim, D.; Takenaka, S.; Yamazaki, H.; Guengerich, F.P.; Shimada, T. Oxidation of Naringenin, Apigenin, and Genistein by Human Family 1 Cytochrome P450 Enzymes and Comparison of Interaction of Apigenin with Human P450 1B1.1 and Scutellaria P450 82D.1. *Chem. Res. Toxicol.* **2023**, *36*, 1778–1788. [[CrossRef](#)]
112. Rendic, S. Summary of information on human CYP enzymes: Human P450 metabolism data. *Drug Metab. Rev.* **2002**, *34*, 83–448. [[CrossRef](#)] [[PubMed](#)]
113. Basheer, L.; Kerem, Z. Interactions between CYP3A4 and Dietary Polyphenols. *Oxid. Med. Cell Longev.* **2015**, *2015*, 854015. [[CrossRef](#)] [[PubMed](#)]
114. Ronis, M.J. Effects of soy containing diet and isoflavones on cytochrome P450 enzyme expression and activity. *Drug Metab. Rev.* **2016**, *48*, 331–341. [[CrossRef](#)] [[PubMed](#)]
115. Chan, H.Y.; Leung, L.K. A potential protective mechanism of soya isoflavones against 7,12-dimethylbenz[a]anthracene tumour initiation. *Br. J. Nutr.* **2003**, *90*, 457–465. [[CrossRef](#)]
116. Omura, T.; Sato, R. The carbon monoxide-binding pigment of liver microsomes. I. Evidence for its hemoprotein nature. *J. Biol. Chem.* **1964**, *239*, 2370–2378. [[CrossRef](#)]
117. Girhard, M.; Klaus, T.; Khatri, Y.; Bernhardt, R.; Urlacher, V.B. Characterization of the versatile monooxygenase CYP109B1 from *Bacillus subtilis*. *Appl. Microbiol. Biotechnol.* **2010**, *87*, 595–607. [[CrossRef](#)]
118. Neunzig, J.; Sanchez-Guijo, A.; Mosa, A.; Hartmann, M.F.; Geyer, J.; Wudy, S.A.; Bernhardt, R. A steroidogenic pathway for sulfonated steroids: The metabolism of pregnenolone sulfate. *J. Steroid Biochem. Mol. Biol.* **2014**, *144 Pt B*, 324–333. [[CrossRef](#)]
119. Mulrooney, S.B.; Waskell, L. High-level expression in *Escherichia coli* and purification of the membrane-bound form of cytochrome b(5). *Protein Expr. Purif.* **2000**, *19*, 173–178. [[CrossRef](#)]
120. Zöllner, A.; Kagawa, N.; Waterman, M.R.; Nonaka, Y.; Takio, K.; Shiro, Y.; Hannemann, F.; Bernhardt, R. Purification and functional characterization of human 11beta hydroxylase expressed in *Escherichia coli*. *FEBS J.* **2008**, *275*, 799–810. [[CrossRef](#)]
121. Kranz-Finger, S.; Mahmoud, O.; Ricklefs, E.; Ditz, N.; Bakkes, P.J.; Urlacher, V.B. Insights into the functional properties of the marneral oxidase CYP71A16 from *Arabidopsis thaliana*. *Biochim. Biophys. Acta Proteins Proteom.* **2018**, *1866*, 2–10. [[CrossRef](#)]
122. Hsu, M.H.; Baer, B.R.; Rettie, A.E.; Johnson, E.F. The Crystal Structure of Cytochrome P450 4B1 (CYP4B1) Monooxygenase Complexed with Octane Discloses Several Structural Adaptations for omega-Hydroxylation. *J. Biol. Chem.* **2017**, *292*, 5610–5621. [[CrossRef](#)]
123. Benkert, P.; Biasini, M.; Schwede, T. Toward the estimation of the absolute quality of individual protein structure models. *Bioinformatics* **2010**, *27*, 343–350. [[CrossRef](#)]
124. Waterhouse, A.; Bertoni, M.; Bienert, S.; Studer, G.; Tauriello, G.; Gumienny, R.; Heer, F.T.; de Beer, T.A.P.; Rempfer, C.; Bordoli, L.; et al. SWISS-MODEL: Homology modelling of protein structures and complexes. *Nucleic Acids Res.* **2018**, *46*, W296–W303. [[CrossRef](#)]
125. Sanner, M.F. Python: A programming language for software integration and development. *J. Mol. Graph. Model.* **1999**, *17*, 57–61.
126. Khatri, Y.; Hannemann, F.; Girhard, M.; Kappl, R.; Hutter, M.; Urlacher, V.B.; Bernhardt, R. A natural heme-signature variant of CYP267A1 from *Sorangium cellulosum* So ce56 executes diverse omega-hydroxylation. *FEBS J.* **2015**, *282*, 74–88. [[CrossRef](#)]
127. Huey, R.; Morris, G.M.; Olson, A.J.; Goodsell, D.S. A semiempirical free energy force field with charge-based desolvation. *J. Comput. Chem.* **2007**, *28*, 1145–1152. [[CrossRef](#)]
128. Morris, G.M.; Goodsell, D.S.; Halliday, R.S.; Huey, R.; Hart, W.E.; Belew, R.K.; Olson, A.J. Automated docking using a Lamarckian genetic algorithm and an empirical binding free energy function. *J. Comput. Chem.* **1998**, *19*, 1639–1662. [[CrossRef](#)]

**Disclaimer/Publisher’s Note:** The statements, opinions and data contained in all publications are solely those of the individual author(s) and contributor(s) and not of MDPI and/or the editor(s). MDPI and/or the editor(s) disclaim responsibility for any injury to people or property resulting from any ideas, methods, instructions or products referred to in the content.